

Extensive Aspartoacylase Expression in the Rat Central Nervous System

JOHN R. MOFFETT,^{1*} PEETHAMBARAN ARUN,¹ PRASANTH S. ARIYANNUR,¹ JAMES Y. GARBERN,² DAVID M. JACOBOWITZ,¹ AND ARYAN M. A. NAMBOODIRI¹

¹Department of Anatomy, Physiology & Genetics, Uniformed Services University of the Health Sciences, Bethesda, Maryland

²Department of Neurology and Center for Translational Neuromedicine, University of Rochester Medical Center, Rochester, New York

KEY WORDS

ASPA; *N*-acetylaspargate; NAA; Canavan disease; oligodendrocytes; microglia; leptomeninges; myelin; acetyl coenzyme A; acetyl coenzyme A synthase; protein acetylation; histone acetylation

ABSTRACT

Aspartoacylase (ASPA) catalyzes deacetylation of *N*-acetylaspargate (NAA) to generate acetate and aspartate. Mutations in the gene for ASPA lead to reduced acetate availability in the CNS during development resulting in the fatal leukodystrophy Canavan disease. Highly specific polyclonal antibodies to ASPA were used to examine CNS expression in adult rats. In white matter, ASPA expression was associated with oligodendrocyte cell bodies, nuclei, and some processes, but showed a dissimilar distribution pattern to myelin basic protein and oligodendrocyte specific protein. Microglia expressed ASPA in all CNS regions examined, as did ependymal cells of the choroid plexus. Pial and ependymal cells and some endothelial cells were ASPA positive, as were unidentified cellular nuclei throughout the CNS. Astrocytes did not express ASPA in their cytoplasm. In some fiber pathways and nerves, particularly in the brainstem and spinal cord, the axoplasm of many neuronal fibers expressed ASPA, as did some neurons. Acetyl coenzyme A synthase immunoreactivity was also observed in the axoplasm of many of the same fiber pathways and nerves. All ASPA-immunoreactive elements were unstained in brain sections from tremor rats, an ASPA-null mutant. The strong expression of ASPA in oligodendrocyte cell bodies is consistent with a lipogenic role in myelination. Strong ASPA expression in cell nuclei is consistent with a role for NAA-derived acetate in nuclear acetylation reactions, including histone acetylation. Expression of ASPA in microglia may indicate a role in lipid synthesis in these cells, whereas expression in axons suggests that some neurons can both synthesize and catabolize NAA. © 2011 Wiley-Liss, Inc.

INTRODUCTION

Aspartoacylase (ASPA, EC 3.5.1.15) is one of three aminoacylase enzymes that are responsible for the deacetylation of *N*-acetylated amino acids. In tissues such as kidney, these acetylated amino acids are derived from the catabolism of *N*-terminal acetylated proteins (reviewed in Perrier et al., 2005), and aminoacylase enzymes act to salvage the deacetylated amino acids for reuse in protein synthesis (Lindner et al., 2008). Amino-

acylases 1 and 3 have relatively broad substrate specificity and act on a number of *N*-acetylated amino acids. ASPA, also known as aminoacylase 2, acts to deacetylate only one acetylated amino acid, namely *N*-acetylaspargate (NAA; D'Adamo et al., 1977; Madhavarao et al., 2003). ASPA hydrolyzes NAA into free acetate and aspartate (Kaul et al., 1993; Zeng et al., 2002) and is expressed strongly in a number of tissues including the brain and kidney (Birnbaum, 1955; Hershfield et al., 2006; Madhavarao et al., 2004). In peripheral tissues, ASPA may function like other aminoacylases to recycle NAA derived from the breakdown of proteins such as actin, which is acetylated at its *N*-terminal aspartate (Alving et al., 1966; Gaetjens et al., 1966). However, in light of the exceptionally high concentration of NAA in the brain (10 mM or higher; Inglese et al., 2008; Miyake et al., 1981; Tallan, 1957), ASPA has apparently adopted additional specialized roles in CNS metabolism beyond simple amino acid salvage associated with the turnover of *N*-acetylated proteins.

Mutations in genes encoding for aminoacylase enzymes lead to reduced or absent capacity for the catabolism of *N*-acetylated amino acids, and increased excretion of the corresponding acetylated amino acids in urine. Mutations in aminoacylase 1 lead to an inborn error of metabolism and result in macrocephaly and neurological symptoms (Sass et al., 2006, 2007). The most severe aminoacylase deficiency results from mutations in the gene that encodes for ASPA, leading to the development of Canavan disease during infancy (Matalon et al., 1988). Canavan disease is a progressive and fatal hereditary neurodegenerative disease characterized by macrocephaly, reduced myelination, and severe vacuolation in thalamus, midbrain, brainstem, and spinal cord (Adachi et al., 1973; Matalon et al., 1995; Surendran et al., 2005). Catabolism of NAA is absent in Canavan disease patients, NAA levels are increased in the

Grant sponsor: MAAN (NIH); Grant number: RO1, NS39387; Grant sponsor: Samuelli Institute; Grant numbers: G170-ON, G170-PI; Grant sponsor: J.R.M.; Grant sponsor: JYG (National Multiple Sclerosis Society); Grant number: RG 3204.

*Correspondence to: John R. Moffett, Department of Anatomy, Physiology & Genetics, Uniformed Services University of the Health Sciences, 4301 Jones Bridge Road, Bethesda, MD 20814, USA. E-mail: jmoffett@usuhs.mil

Received 9 November 2010; Accepted 14 April 2011

DOI 10.1002/glia.21186

Published online in Wiley Online Library (wileyonlinelibrary.com).

Report Documentation Page

Form Approved
OMB No. 0704-0188

Public reporting burden for the collection of information is estimated to average 1 hour per response, including the time for reviewing instructions, searching existing data sources, gathering and maintaining the data needed, and completing and reviewing the collection of information. Send comments regarding this burden estimate or any other aspect of this collection of information, including suggestions for reducing this burden, to Washington Headquarters Services, Directorate for Information Operations and Reports, 1215 Jefferson Davis Highway, Suite 1204, Arlington VA 22202-4302. Respondents should be aware that notwithstanding any other provision of law, no person shall be subject to a penalty for failing to comply with a collection of information if it does not display a currently valid OMB control number.

1. REPORT DATE 2011	2. REPORT TYPE	3. DATES COVERED
4. TITLE AND SUBTITLE Extensive Aspartoacylase Expression In The Rat Central Nervous System		5a. CONTRACT NUMBER
		5b. GRANT NUMBER
		5c. PROGRAM ELEMENT NUMBER
6. AUTHOR(S)		5d. PROJECT NUMBER
		5e. TASK NUMBER
		5f. WORK UNIT NUMBER
7. PERFORMING ORGANIZATION NAME(S) AND ADDRESS(ES) Uniformed Services University of the Health Sciences, Department of Anatomy, Physiology & Genetics, Bethesda, MD, 20814		8. PERFORMING ORGANIZATION REPORT NUMBER
9. SPONSORING/MONITORING AGENCY NAME(S) AND ADDRESS(ES)		10. SPONSOR/MONITOR'S ACRONYM(S)
		11. SPONSOR/MONITOR'S REPORT NUMBER(S)
12. DISTRIBUTION/AVAILABILITY STATEMENT Approved for public release; distribution unlimited.		
13. SUPPLEMENTARY NOTES The original document contains color images.		
14. ABSTRACT Aspartoacylase (ASPA) catalyzes deacetylation of N-acetylaspartate (NAA) to generate acetate and aspartate. Mutations in the gene for ASPA lead to reduced acetate availability in the CNS during development resulting in the fatal leukodystrophy Canavan disease. Highly specific polyclonal antibodies to ASPA were used to examine CNS expression in adult rats. In white matter, ASPA expression was associated with oligodendrocyte cell bodies, nuclei, and some processes, but showed a dissimilar distribution pattern to myelin basic protein and oligodendrocyte specific protein. Microglia expressed ASPA in all CNS regions examined, as did ependymal cells of the choroid plexus. Pia and ependymal cells and some endothelial cells were ASPA positive, as were unidentified cellular nuclei throughout the CNS. Astrocytes did not express ASPA in their cytoplasm. In some fiber pathways and nerves, particularly in the brainstem and spinal cord, the axoplasm of many neuronal fibers expressed ASPA, as did some neurons. Acetyl coenzyme A synthase immunoreactivity was also observed in the axoplasm of many of the same fiber pathways and nerves. All ASPA-immunoreactive elements were unstained in brain sections from tremor rats, an ASPA-null mutant. The strong expression of ASPA in oligodendrocyte cell bodies is consistent with a lipogenic role in myelination. Strong ASPA expression in cell nuclei is consistent with a role for NAA-derived acetate in nuclear acetylation reactions, including histone acetylation. Expression of ASPA in microglia may indicate a role in lipid synthesis in these cells, whereas expression in axons suggests that some neurons can both synthesize and catabolize NAA.		
15. SUBJECT TERMS		

16. SECURITY CLASSIFICATION OF:			17. LIMITATION OF ABSTRACT	18. NUMBER OF PAGES 22	19a. NAME OF RESPONSIBLE PERSON
a. REPORT unclassified	b. ABSTRACT unclassified	c. THIS PAGE unclassified			

Standard Form 298 (Rev. 8-98)
Prescribed by ANSI Std Z39-18

brain, and affected neonates excrete excess NAA in their urine (Jakobs et al., 1991; Kelley et al., 1992).

The primary functional significance of ASPA-mediated deacetylation of NAA in the CNS is still under debate after decades of research, and there is additional uncertainty concerning the metabolic fate of the acetate derived from NAA catabolism (reviewed in Moffett et al., 2007). Acetyl coenzyme A (acetyl CoA) is a primary building block for lipids, and ASPA-mediated deacetylation of NAA has been proposed to provide some of the acetate necessary for the synthesis of acetyl CoA, and in turn myelin lipids (Burri et al., 1991; D'Adamo et al., 1966, 1968; Mehta et al., 1995; Namboodiri et al., 2006). Therefore, Canavan disease has been hypothesized to result from a deficiency in NAA-derived acetate, which leads to decreased myelin synthesis during early post-natal CNS development (Hagenfeldt et al., 1987; Madhavarao et al., 2005; Mehta et al., 1995; Wang et al., 2009). Other metabolic deficits that may result from ASPA deficiency include virtually all cellular functions linked to acetyl CoA supply in the CNS, particularly in oligodendrocytes. These could include protein acetylation reactions such as nuclear histone acetylation, endoplasmic reticulum protein acetylation and cytoskeletal protein acetylation (Ariyannur et al., 2010b). ASPA is localized in both the cytosolic and nuclear compartments of oligodendrocytes and is transported between the two compartments (Hershfield et al., 2006). Additionally, one of the enzymes responsible for converting free acetate derived from NAA into acetyl coenzyme A, known as acetyl coenzyme A synthase-1 (AceCS1), is also localized in the nuclei of oligodendrocytes (Ariyannur et al., 2010a). The localization pattern for these two enzymes is consistent with a role for NAA-derived acetate in nuclear histone acetylation reactions in oligodendrocytes. Histone acetylation is associated with epigenetic gene regulation, and therefore disrupted histone acetylation in Canavan disease may be a major etiological factor in the progression of the disease.

The polyclonal antibody used in the current study, which was directed against an ASPA peptide sequence, provided an expanded and more detailed expression pattern for ASPA than reported in previous studies. Most importantly, in the current study the identity of the target epitope was confirmed to correspond exclusively to ASPA protein by demonstrating that no staining was present in brain tissue sections from a mutant rat strain, the tremor rat, in which the ASPA gene sequence is absent (Kitada et al., 2000). Here, we present a detailed analysis of ASPA protein expression throughout the rat brain.

MATERIALS AND METHODS

ASPA Antibodies

Specific rabbit polyclonal antibodies were produced against a 19 amino acid conserved murine and human ASPA peptide sequence (residues 83-101: SEDLPYEV-RAQEINHLFG). This antibody has been reported previ-

ously (Hershfield et al., 2006). During the course of working with the polyclonal anti-ASPA sera it was found that diffuse background staining occurred in wild type and tremor rat tissue sections. To remove non-specific antibodies, polyclonal antisera were diluted 1:1,000 in PBS containing 2% normal goat serum (NGS) and pre-incubated for 24 h or longer with an excess of formalin-fixed liver and brain tissue slices from tremor rats. This process was repeated until no background immunoreactivity was observed in tremor rat brain slices.

Peroxidase Immunohistochemistry

Six adult female and three adult male Sprague-Dawley rats (Charles River Laboratories, Raleigh, NC, 200–250 g) and three tremor rats (Wistar strain, 70 days old, bred in our facility) were anesthetized with pentobarbital (50 mg/kg) and perfused transcardially with 400 mL of 4% freshly depolymerized paraformaldehyde. Brains were removed and postfixed for several hours in paraformaldehyde before being passed through a series of 10%, 20%, and 30% sucrose solutions. Brains were grossly cut in 4 mm thick coronal blocks using a Jacobowitz rat brain matrix slicer (Jacobowitz, 1974) and the blocks were mounted on aluminum chucks in OCT embedding compound and frozen rapidly with compressed difluoroethane gas. Coronal sections were cut at a thickness of 20 μ m at -18° C and were collected in 10 mM phosphate buffered saline (PBS).

Avidin-biotin complex/oxidase immunohistochemistry was done as previously described (Madhavarao et al., 2004) with some modifications. Sections were processed free-floating. Endogenous peroxidase activity was blocked by washing freshly cut sections in PBS and incubating them in a 50:50 mixture of methanol and water containing 1% H_2O_2 for 30 min. Sections were blocked against non-specific antibody binding by incubation for 20 min or longer in PBS containing 2% NGS and 0.1% sodium azide.

Brain sections were incubated for 16–24 h with the tremor tissue-adsorbed polyclonal ASPA antibodies at a dilution of 1:25,000–1:30,000. Sections were maintained in a humid chamber at room temperature with constant rotary agitation, and were washed thoroughly after incubation to remove sodium azide. Bound antibodies were visualized by the avidin-biotin complex method with horseradish peroxidase as the enzyme marker (Vectastain Elite; Vector Labs, Burlingame, CA). The sections were incubated with the biotinylated secondary antibody and avidin-peroxidase complex solutions for 90 min each. The secondary antibody was diluted in PBS plus 2% NGS and the ABC reagent in PBS plus 0.5% BSA, both without azide. After final washing, the sections were developed with a Ni and Co enhanced diaminobenzidine chromogen (Pierce Chemical, Rockford, IL). AceCS1 immunohistochemistry was performed as previously described (Ariyannur et al., 2010a).

Comparative studies with antibodies to myelin basic protein (MBP) and oligodendrocyte specific protein

(OSP) were done by a modified method to improve antibody penetration into dense myelin. Antigen retrieval was performed on free floating tissue sections using EDTA (5 mM HEPES buffer with 1 mM EDTA and 0.05% Triton X-100 at pH 8 and 80°C for 10 min). Polyclonal antibodies (Abcam, Cambridge, MA; MBP = #AB 2404; OSP = #AB 53041) were diluted 1:500, and 1:4,000, respectively, and purified ASPA antibodies were diluted 1:30,000. Primary antibodies were applied to tissue sections for 42–48 h at room temperature in a humid chamber with constant rotary agitation. Incubation times with the biotinylated secondary antibody and avidin-peroxidase complex were extended to 2 h each.

Stained sections were transferred to deionized water containing 0.01% BSA, and were manually mounted on treated slides (Superfrost plus, Fischer Scientific) with a fine tipped brush. Slides were dried at 45°C for 10 to 15 min, dehydrated in an ethanol series, cleared in xylene and sealed with cover glasses using xylene based adhesive. Images were acquired on a DIC-equipped Olympus BX51 microscope with an Olympus DP71 digital camera, and were adjusted to normalize brightness and contrast with PC based imaging software (Adobe Systems, San Jose, CA). Additional software was used to correct for background illumination levels, and in some cases to produce images with extended depth of field (Media Cybernetics, Silver Spring, MD).

Protein Extract Preparation for Western Blotting

Two adult Sprague-Dawley wild-type rats and two tremor rats were euthanized, brains were removed and frozen on dry ice, and stored at -80°C until use. All subsequent steps were performed on ice. Tissues were minced and homogenates were prepared by 8–10 strokes with a Potter-Elvehjem homogenizer in isolation medium (0.25 M sucrose, 25 mM KCl, 5 mM MgCl_2 , 10 mM Tris-HCl, pH 7.4) with protease inhibitor cocktail (15 $\mu\text{L}/\text{mL}$) and phosphatase inhibitors (Sigma-Aldrich). Following filtration, solutions were centrifuged (800 g, 10 min 4°C), the supernatants were adjusted to homogenization buffer (0.5 mM DTT, 50 mM Tris-HCl, pH 8.0, 50 mM NaCl, 0.05% IGEPAL CA-630, 8% glycerol) and were centrifuged again (16,000g, 20 min, 4°C). The resulting supernatants were used for Western blotting. Protein concentrations were determined by Bio-Rad's DC protein assay (Hercules, CA).

SDS-PAGE and Western Blot

Western blotting was done as previously described (Ariyannur et al., 2010a). Samples were diluted in loading buffer with 10 mM DTT, and heated (90°C , 5 min) before loading onto 10% pre-cast Tris-glycine gels (Invitrogen, Carlsbad, CA). Brain proteins were applied at 60 μg per lane. Proteins were transferred to Immobilon-P PVDF membranes, which were blocked with 0.05% Tween-20 and 5% NGS. Blots were incubated overnight

with anti-ASPA antibodies (see figure legend for antibody concentrations), were washed in PBS, and then incubated for 1 h with horseradish peroxidase-conjugated secondary antibodies (1:2,500). Membranes were washed with PBS and developed with Sigma Fast diaminobenzidine substrate (Sigma/Aldrich).

RESULTS

ASPA Antibody Specificity

In the current study, we have examined the cellular localization of ASPA protein in the rat CNS using an adsorption purified polyclonal antibody. The crude polyclonal antibody was specific for ASPA, and displayed a major protein band with an apparent molecular weight of ~ 37 kDa in Western blots of the protein extracts from rat brain homogenates (Fig. 1 insert). Two relatively minor immunoreactive bands were observed at other molecular weights in Western blots of protein extracts from wild type and tremor rat brains with unpurified antisera. After adsorption of the crude ASPA antisera with brain and liver tissue from tremor rats, the non-specific immunoreactive bands were absent in Western blots, and only the 37 kDa band remained with brain extracts from wild type rats.

Using the crude antisera, we observed non-specific background staining in brain sections from wild type and tremor rats at the dilutions used for immunohistochemistry (1:25,000–1:30,000). The background staining was especially strong in the striatum (Fig. 1A,B), and it was determined that this background staining could be removed by pre-incubating partially diluted antisera with formalin-fixed brain and liver tissue slices from tremor rats. Pre-incubation of the polyclonal antibodies with a large excess of tissue sections from this ASPA null animal removed the non-specific antibodies from the polyclonal mixture (Fig. 1C,D). Using this method we were able to produce highly specific polyclonal antibody preparations with virtually no background staining, providing high-contrast images with exceptional cellular detail. This adsorption purification method also prevented the typical loss of antibody titer associated with affinity purification. Further, all immunoreactivity with the pre-adsorbed anti-ASPA antibodies was absent in tremor rat brain sections (Fig. 1D), indicating that all immunoreactivity in wild type rat brain sections was due to ASPA protein expression.

ASPA Immunoreactivity Overview

In general, ASPA immunoreactivity in the brain was most intense in fiber tracts, thalamus and brainstem as previously reported (Klugmann et al., 2003; Madhavarao et al., 2004). Cortical areas including isocortex, hippocampus, piriform cortex, entorhinal cortex and cerebellar cortex had generally lower expression levels for ASPA than white matter. Fiber tract ASPA expression was predominated by oligodendrocytes, whereas expres-

sion in gray matter occurred in oligodendrocytes, microglia and unidentified cellular nuclei. In addition to oligodendrocytes and microglia, pial cells were among the most strongly immunoreactive cells for ASPA throughout the brain. We also found that ASPA expression was stronger in fiber pathways than could be accounted for by oligodendrocytes and their processes. In forebrain, fiber pathways such as the corpus callosum, fornix, optic chiasm and tracts, internal capsule and medial forebrain

bundle all showed light to moderate ASPA immunoreactivity in apparent axons, but this was difficult to image at the light microscopic level due to the high level of expression in oligodendrocytes and some of their processes. Axoplasmic ASPA expression was more obvious in large diameter fibers of the brainstem. When caudal fiber pathways composed of large axons were cut in cross section the axoplasm was immunoreactive, but the myelin sheaths were unstained.

Another notable aspect of ASPA expression was the clear demarcation of differential oligodendrocyte morphologies associated with fiber tracts composed of small diameter fibers versus those composed of large diameter fibers. Oligodendrocytes have been classified according to their morphology and the number and size of neuronal fibers they myelinate. Types I and II oligodendrocytes predominate in forebrain pathways such as corpus callosum, where fiber diameters rarely exceed 2 μm in diameter, whereas in hindbrain and spinal cord, Types III and IV oligodendrocytes predominate where axon diameters often reach 4 μm or greater in diameter (Butt et al., 1998). Type I/II oligodendrocytes typically myelinate multiple smaller diameter axons, whereas Type III/IV oligodendrocytes usually myelinate a single large diameter axon. ASPA expression clearly demonstrated two very different morphologies among oligodendrocytes. Consistent with the Type I/II morphology, oligodendrocytes in many forebrain pathways such as corpus callosum, anterior commissure, internal capsule and olfactory tracts all had relatively small cell bodies and multiple proximal processes that branched. In contrast, many oligodendrocytes in more posterior pathways containing larger diameter axonal fibers had larger cell bodies, and often had one very large proximal process which did not branch, which is consistent with a Type III/IV morphology.

ASPA Expression by Region

In the telencephalon ASPA expression was most prominent in fiber tracts. Immunoreactivity in cortical areas was lower in comparison to white matter, as previously reported (Kaul et al., 1991; Madhavarao et al., 2004) but was still substantial. In isocortex ASPA was expressed predominantly in three cell types, pial cells at the sur-

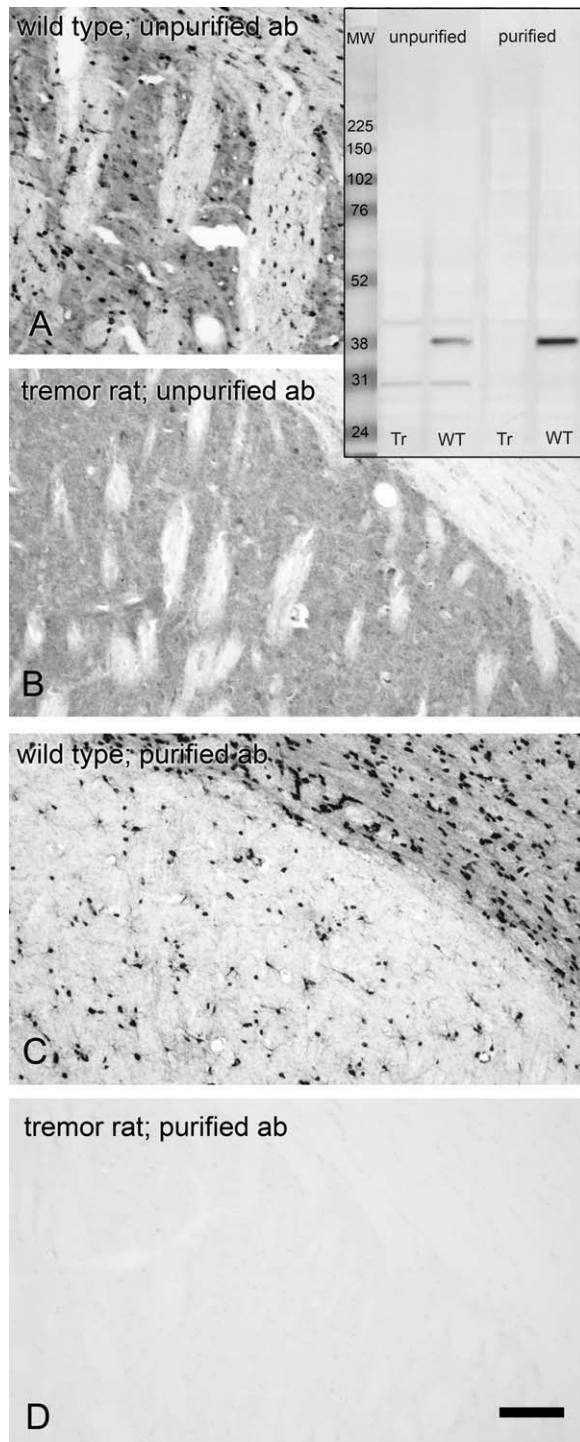


Fig. 1. Antibody purification and specificity. Inset: Western blots of brain protein extracts from tremor (Tr) and wild-type (WT) rats. Crude antiserum was diluted 1:25,000 (left two lanes), purified antiserum (tremor tissue adsorbed) was diluted 1:15,000 (right two lanes). In addition to the major band at 37 kD in the wild-type rats, several minor bands were present with the crude sera in both tremor and wild-type rat homogenates. Only one band was present in the wild-type extracts after antibody purification, and no significant bands were seen in the tremor rat extracts (MW, molecular weight markers; values in kDa). Panels A through D show the striatum and corpus callosum in normal and tremor rats stained with crude antiserum versus antiserum purified by preadsorption with tremor rat tissue. A: Wild-type rat forebrain tissue stained with crude antibody at a dilution of 1:20,000. B: Tremor rat forebrain tissue stained with crude antibody at a dilution of 1:20,000. C: Wild-type rat forebrain tissue stained with pre-adsorbed antibody at a dilution of 1:30,000. D: Tremor rat forebrain tissue stained with pre-adsorbed antibody at a dilution of 1:30,000. Scale Bar = 120 μm .

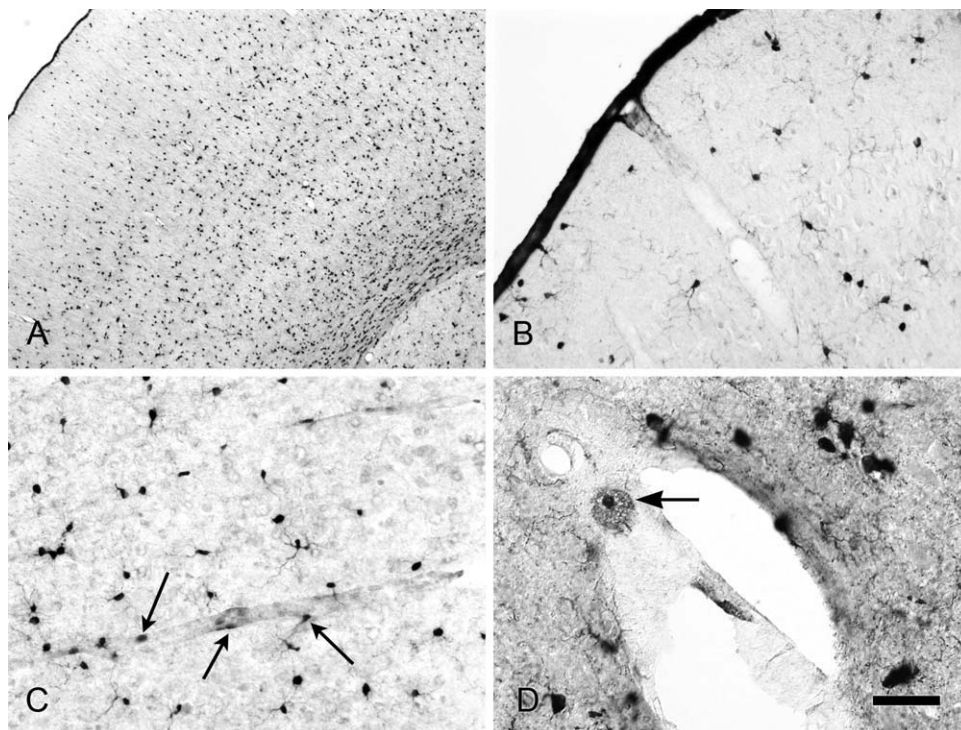


Fig. 2. Cortex, meninges, and vasculature. ASPA expression in somatosensory cortex showing the distribution of ASPA-positive cells (A). Strong ASPA expression was observed in the pia matter at the cortical surface, and lower immunoreactivity was associated with the initial portion of a penetrating blood vessel (B). A lightly immunoreac-

tive blood vessel is shown in neocortical Layers II/III (C, immunoreactive endothelial cell nuclei shown by arrows). An immunoreactive blood vessel in Layers III/IV (D). Endothelial cell in a vessel wall expressing ASPA lightly in the cytoplasm and moderately in the nucleus. Scale bar = 300 μ m A, 60 μ m B and C, and 30 μ m D (DIC optics D).

face, microglia in all cortical layers, and oligodendrocytes located most extensively in the deeper layers. At the cortical surface ASPA was expressed very strongly in cells of the pia mater (Fig. 2A,B). The pial cells were intensely stained in both nucleus and cytoplasm. Pia mater is comprised of pial cells, extracellular collagen fibrils, and meningeal macrophages. The strong ASPA expression in pia mater transitioned to very light expression in the tunica externa surrounding some arterioles penetrating the cortical surface (Fig. 2B). Some blood vessels throughout the brain were lightly immunoreactive for ASPA, and in many cases the endothelial cell nuclei were more strongly stained than their cytoplasm (Fig. 2C,D).

Isocortex

ASPA expression in isocortex was distributed in all layers (Fig. 3A). In isocortical Layers I through III most ASPA expression was observed in microglia. ASPA-expressing microglia were highly ramified in morphology, typically issuing several major processes, which branched further at their distal ends forming a network of fine immunoreactive fibers throughout the neuropil. Layer I of isocortex contained scattered immunoreactive microglial cells (Fig. 3B). In addition to ramified microglia, a few strongly immunoreactive cells in Layer I had the appearance of oligodendrocytes (Fig. 3B, arrow). Oligodendrocyte specific protein (OSP) immunoreactivity was observed in

a network of very fine diameter oligodendrocyte fibers in Layer I of isocortex (Fig. 3C). Myelin basic protein (MBP) was also observed in a network of lightly myelinated fibers in isocortical Layer I, and these were of larger diameter than the fibers stained for OSP (Fig. 3D). Isocortical Layers II and III contained many ASPA-positive microglia and an associated network of their immunoreactive processes. In Layers IV through VI, numerous APSA-positive oligodendrocytes were the predominant immunoreactive cell type, and were intermingled with immunoreactive microglia. This increasing protein expression of ASPA from cortical surface to the underlying white matter is also reflected in ASPA enzyme assays showing increasing activity in tissue homogenates taken from superficial to deep layers of isocortex (Kaul et al., 1991). Finally, as was observed throughout the CNS, many cellular nuclei from unidentified cell types were lightly to moderately ASPA positive in all cortical layers. These ASPA expressing cell nuclei were relatively small in size (typically 4–7 μ m in the longest dimension) indicating that many of them likely belonged to glial cells. Future dual labeling immunofluorescence experiments using markers for neurons and various glial cell types are warranted.

Comparison with Expression of Other Oligodendrocyte Markers

After mild antigen retrieval MBP immunoreactivity was greatly increased throughout the CNS. OSP immu-

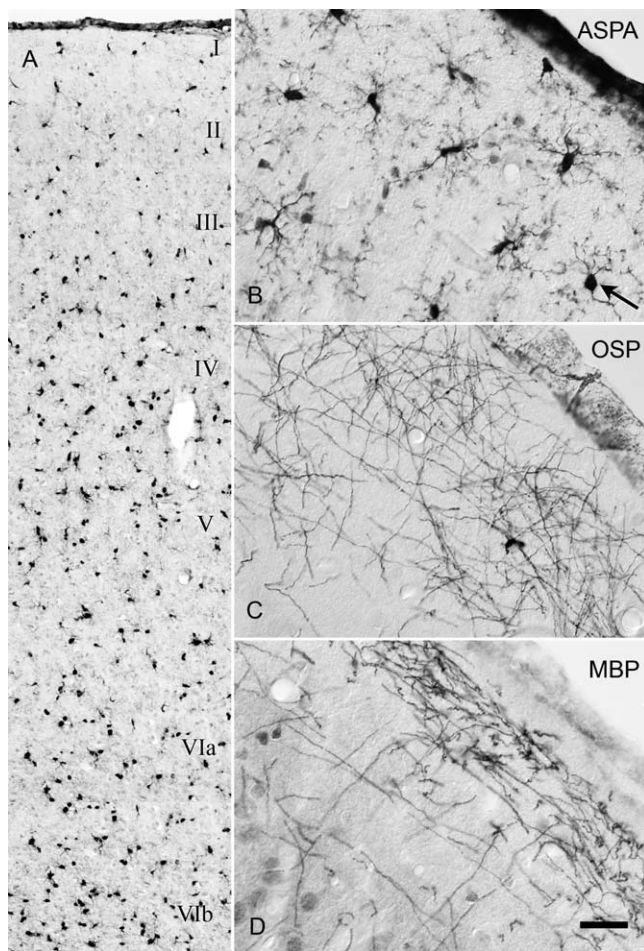


Fig. 3. Somatosensory cortex. All layers of rat somatosensory cortex are shown in **A**. Very strong ASPA immunoreactivity was present in the pia matter, with sparser expression in cortical Layers I through III. The greatest density of immunoreactive cells was present in Layers IV, V, and deeper portions of Layer VI. ASPA expression in Layer I of isocortex was predominated by apparent microglia with a smaller population of oligodendrocytes (e.g., arrow in **B**). In contrast to ASPA expression in oligodendrocyte and microglial cell bodies and some processes, oligodendrocyte specific protein (OSP) was present in a network of very fine diameter oligodendrocyte processes in Layer I of cortex, where an occasional OSP-positive cell body was also observed (**C**). Myelin basic protein (MBP) immunoreactivity in Layer I of cortex was present in a network of fibers that were of larger diameter than those seen with OSP (**D**). Antigen retrieval was used in B–D. Scale bar = 120 μ m A and 20 μ m B–D.

nonreactivity was also substantially increased, whereas ASPA immunoreactivity was more modestly improved. The staining pattern for ASPA in the external capsule and overlying cortex (Fig. 4A,B) was dissimilar to that of OSP (Fig. 4C,D) and MBP (Fig. 4E,F). OSP expression was observed in a dense network of very fine oligodendrocyte processes throughout gray and white matter (Fig. 4C). In Layer V of isocortex, OSP was observed in numerous fine diameter oligodendrocyte processes, with many processes being clustered and arranged in columns (Fig. 4D). MBP immunoreactivity was present in myelin sheaths, and accordingly was more intense in white matter than in gray matter (Fig. 4E). In isocortex, MBP-immunoreactivity was also somewhat concentrated in col-

umns (Fig. 4F). The pattern of fiber staining for MBP had a distinctive appearance from the staining patterns observed with OSP and ASPA antibodies. MBP staining in myelin appeared as patchy immunoreactivity on hollow tubes associated with neuronal axons (Fig. 4F, inset).

Overall, the staining patterns for the three proteins were disparate. ASPA was present in oligodendrocyte cell bodies, nuclei and some processes, especially larger diameter proximal processes. ASPA was also present in microglia and their processes. OSP was present in many more oligodendrocyte processes than seen with ASPA antibodies, but staining was mostly restricted to finer diameter terminal processes, and was only seen in oligodendrocyte cell bodies relatively rarely. The MBP staining pattern shared some similarities to that of OSP, but the diameter of the stained fibers was greater with MBP (myelinated axons) than OSP antibodies (oligodendrocyte processes).

Telencephalic Nuclei

In the septum, caudate-putamen (CP), globus pallidus (GP) and ventral striatum, ASPA was expressed in numerous oligodendrocytes associated with fiber pathways such as the internal capsule, fornix and anterior commissure (ac; Fig. 5A). These forebrain pathways contained predominantly Type I/II oligodendrocytes which issued several processes. Expression of ASPA was more pronounced in the globus pallidus than in the striatum due to the greater density of myelinated fibers (Fig. 5B–D). Immunoreactive microglia were present throughout these areas, and were most apparent in gray matter. In the striatum, ASPA-expressing oligodendrocytes were associated with fiber bundles of the internal capsule (Fig. 5E). The medial septum contained numerous immunoreactive oligodendrocytes associated with the intercalated fibers of the fornix (Fig. 5F). Numerous ASPA-positive cell nuclei were observed throughout the telencephalic nuclei, but due to a lack of cytoplasmic staining their identity could not be determined.

Telencephalic Fiber Pathways

In the corpus callosum most if not all oligodendrocytes were immunoreactive for ASPA to some degree, ranging from very lightly to intensely stained (cc in Fig. 6A, see also Figs. 2A, 5A, and 7A). The great majority of immunoreactive oligodendrocytes in the corpus callosum and external capsule were Type I/II morphologically, with more than one cellular process. ASPA was expressed in oligodendrocyte cell bodies, nuclei, proximal processes, and in some finer more distal processes, but it was not expressed throughout entire oligodendrocyte arborizations. In addition to the corpus callosum, all telencephalic fiber pathways contained numerous oligodendrocytes that expressed ASPA protein, including the fornix (Fig. 6A), fimbria (Fig. 6B), anterior commissure (Fig. 6A,C), lateral olfactory tract (Fig. 6D), internal capsule and stria terminalis (Fig. 6E) and cerebral peduncles

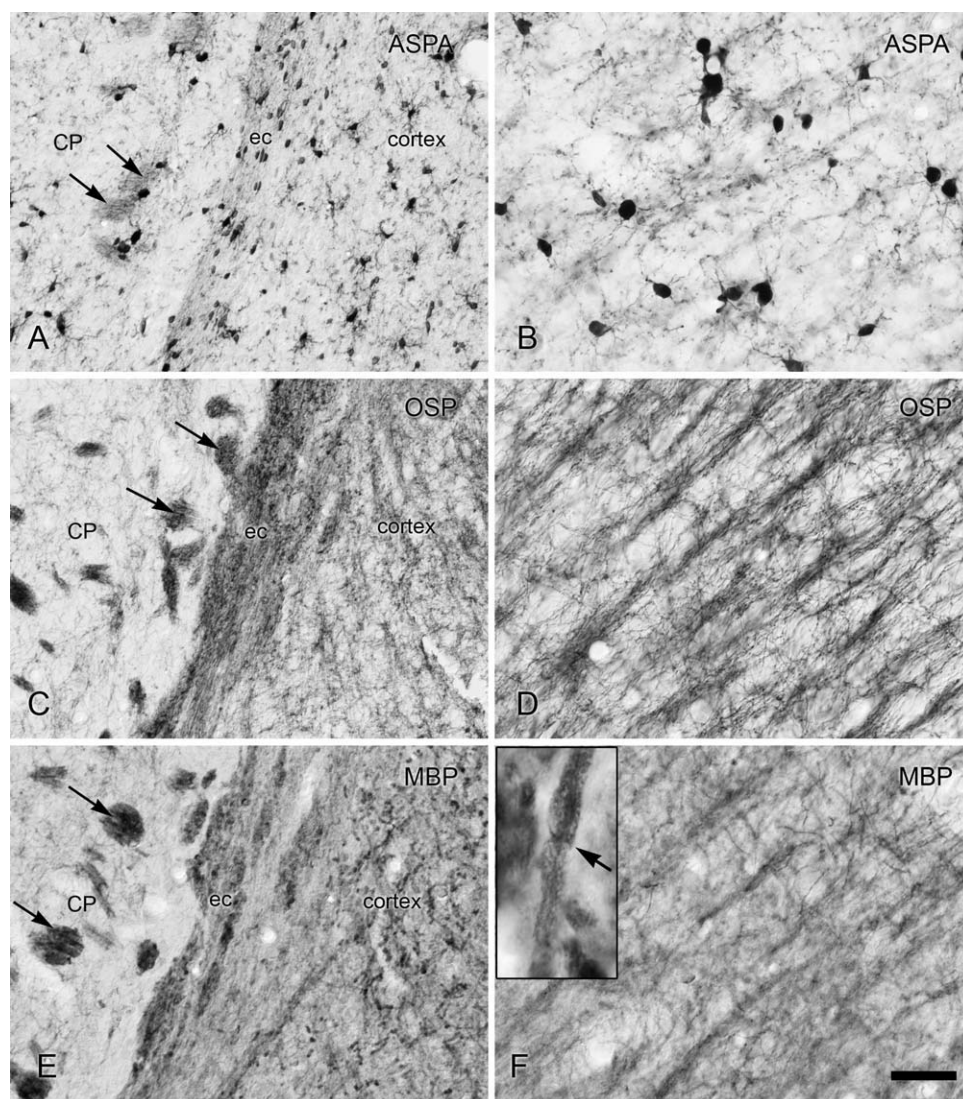


Fig. 4. Comparison with expression of other oligodendrocyte markers. The external capsule (ec) and deeper layers of isocortex contained many oligodendrocytes and microglia that expressed ASPA strongly in their cytoplasm and nuclei (A). In addition to oligodendrocyte and microglial cell bodies, a network of oligodendrocyte and microglial processes expressed ASPA in cortical regions, for example Layer V of isocortex (B). Oligodendrocyte specific protein (OSP) immunoreactivity was present in a denser network of very fine oligodendrocyte processes in both white and

gray matter (C, external capsule and D, Layer V of isocortex). Immunoreactivity for myelin basic protein (MBP) was present only in myelin (E, external capsule and F, Layer V of isocortex). At high magnification, MBP was observed exclusively in ensheathing myelin, where nodes of Ranvier could be identified (arrow; inset in panel F). Arrows in panels A, C, and E show fascicles of the internal capsule. Antigen retrieval was used for all images. ec, external capsule; CP, caudate/putamen. Scale bar = 60 μ m A, C, and E, 30 μ m B, D, and F, 7 μ m inset in F (DIC optics).

(Fig. 6F). Many of the oligodendrocytes in these fore-brain pathways exhibited Type I/II morphology, and were often arranged in rows or clusters with oligodendrocyte cell bodies in direct contact with one another.

The subfornical organ is a circumventricular organ that is outside the blood brain barrier. It contained numerous ASPA immunoreactive microglia with a relatively compact ramified morphology (Fig. 6A, inset). The subfornical organ also contained numerous ASPA-positive cell nuclei which could not be positively identified due to a lack of cytoplasmic staining (Fig. 6A, arrow in inset). The fenestrated vasculature of the subfornical organ was invested with numerous ASPA-positive cells

that included endothelia, microglia and possibly pericytes which surrounded the vessels.

Hippocampus

In the hippocampal formation, ASPA expression was relatively light, and was observed predominantly in microglia and oligodendrocytes. ASPA expressing oligodendrocytes in the hippocampus were densely packed throughout the alveus, fimbria (Figs. 6B and 7A) and fornix (Fig. 6A). Stained oligodendrocytes were also present in the stratum lacunosum moleculare, which contains myelinated axons from hippocampal pyramidal

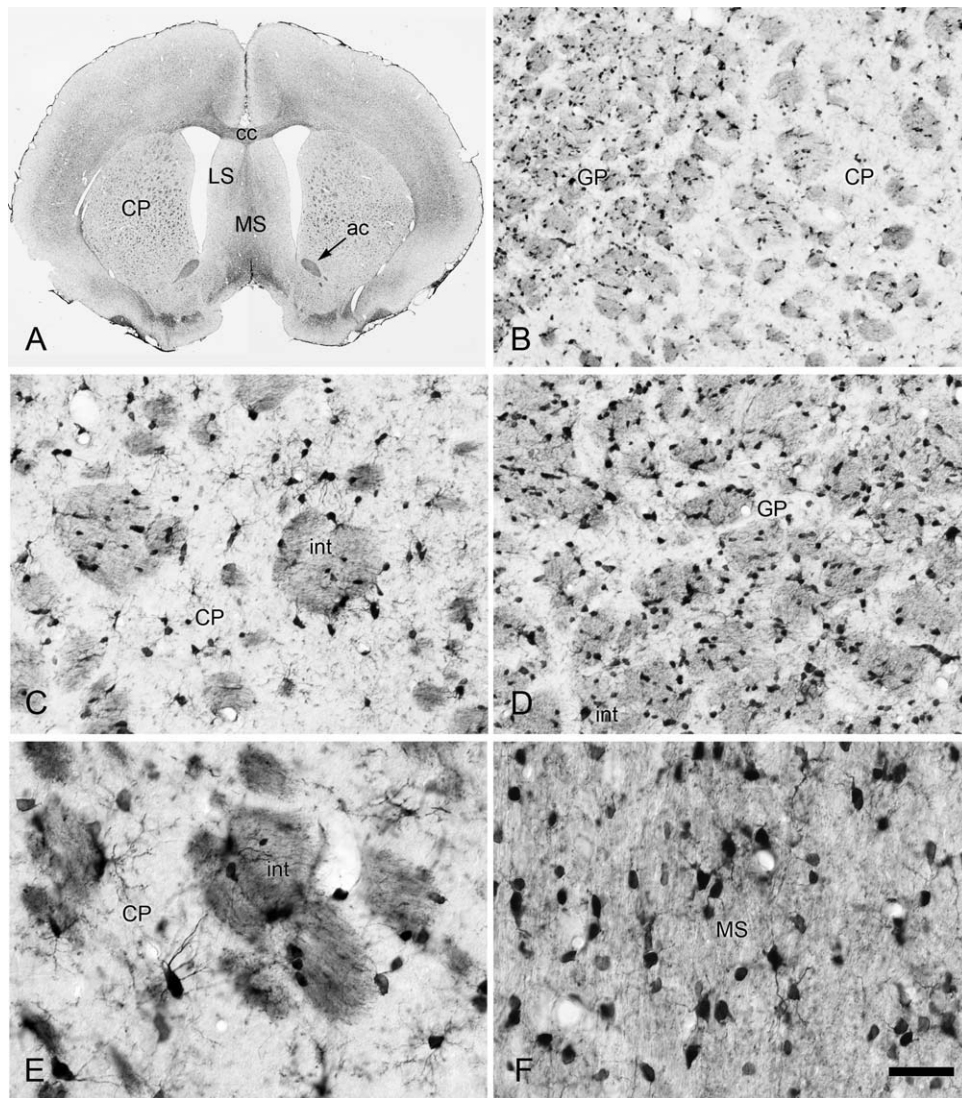


Fig. 5. Telencephalic nuclei. ASPA was expressed strongly in white matter (A). Expression was stronger in nuclear groups that contained numerous myelinated fibers, such as the medial septum (A and F) and globus pallidus (B and D). In the caudate/putamen (CP) strongly immunoreactive oligodendrocytes were clustered in fiber bundles of the inter-

nal capsule (int; C and E). Immunoreactive microglia were observed in all areas. All images are from tissue sections treated for antigen retrieval. ac, anterior commissure; cc, corpus callosum; CP, caudate putamen; GP, globus pallidus; int, internal capsule; LS, lateral septum; MS, medial septum. Scale bar = 2 mm A, 300 μ m B, 120 μ m C and D, 30 μ m E and F.

cells. The most numerous ASPA expressing cells in the hippocampal gray matter were microglia, which were present in large numbers throughout the hippocampal formation (Fig. 7B–F). Microglia in the hippocampus ranged from lightly to strongly immunoreactive and were present in all layers (Fig. 7B), and tended to be more strongly immunoreactive in their cytoplasm than in their nuclei (Fig. 7C, arrow). However, many microglia expressed ASPA in both cytoplasm and nucleus as was the case with other immunoreactive cell types. ASPA-expressing microglia in the hippocampus possessed highly ramified processes which formed a network of fine immunoreactive fibers present throughout the neuropil. The lowest density of ASPA-positive microglia in the hippocampus was observed in the granule cell layer (Fig. 7D).

Thalamus and Hypothalamus

ASPA expression was strong in the thalamus and hypothalamus due to the large number of oligodendrocytes associated with afferent, efferent and en passant fiber pathways. Extensive oligodendrocyte ASPA expression was observed in many nuclear groups, as well as in fiber pathways such as the optic tracts, stria medularis thalami and medial lemniscus, external medullary lamina and posterior commissure (Fig. 8A). In the posterior commissure some oligodendrocytes had larger cell bodies than those observed in forebrain pathways such as corpus callosum, possessing large primary processes directed vertically in the commissure indicative of Type III/IV oligodendrocytes. The optic tracts contained some oligodendrocytes with very large primary processes ori-

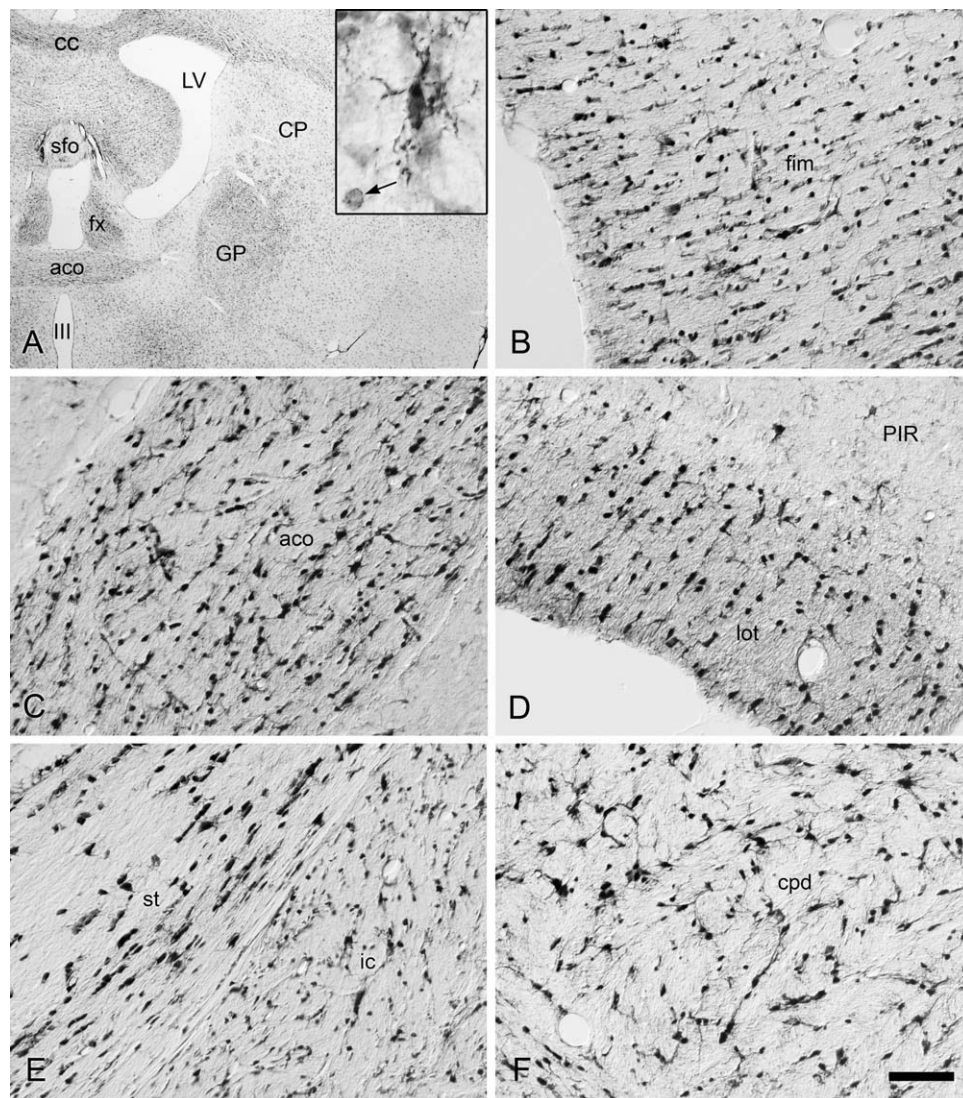


Fig. 6. Telencephalic fiber pathways. Several forebrain fiber pathways are shown in panel (A) including the corpus callosum (cc), anterior commissure (see also C; aco), and fornix (fx). The subfornical organ (sfo) contained many ASPA expressing microglia (A, inset) and many unidentified cell nuclei stained for ASPA (A, arrow in inset). Oligodendrocytes strongly

expressed ASPA in all forebrain fiber pathways such as the fimbria (B; fim), lateral olfactory tract (D; lot), stria terminalis (E; st), and cerebral peduncle (F; cpd). CP, caudate/putamen; GP, globus pallidus; ic, internal capsule; III, third ventricle; LV, lateral ventricle; PIR, piriform cortex. Scale bar = 1 mm A, 15 μ m inset in A, and 60 μ m B–F (DIC optics B–F).

ented perpendicular to the optic fibers (Fig. 8C). The optic chiasm contained numerous ASPA positive oligodendrocytes in a network of fine immunoreactive processes (Fig. 8D). ASPA expression immediately surrounding the III ventricle was relatively sparse, and was predominated by immunoreactive microglia and unidentified cell nuclei (Fig. 8E). Some immunoreactive microglial cells were adherent to the abluminal surface of the ependymal cell layer lining the ventricle. The ependymal cells were lightly stained in their cytoplasm, and some had moderately stained nuclei. The lateral hypothalamus contained numerous strongly immunoreactive oligodendrocytes associated with the medial forebrain bundle (Fig. 8F). At high magnification, the axoplasm of many of the fibers of the medial forebrain bundle was lightly to moderately immunoreactive for ASPA, but their myelin sheaths appeared unstained (Fig.

8F, inset). However, delicate oligodendrocyte processes were immunoreactive at the periphery of myelin sheaths, possibly in the terminal portions of the oligodendrocyte dendrites, or in paranodal oligodendrocyte cytoplasm.

Midbrain

ASPA expression in the midbrain was strongest in areas with high densities of myelinated fibers. ASPA expression in the periaqueductal gray was relatively light (Fig. 9A) with microglia being the most commonly stained elements there. Expression was also modest in the superficial gray matter layers of the superior colliculus, but was more pronounced in deeper layers (Fig. 9B). ASPA expression was also relatively low in the reticular portion of the substantia nigra (Fig. 9A,C). The central roots of the third cranial nerve (n III; oculomotor) were

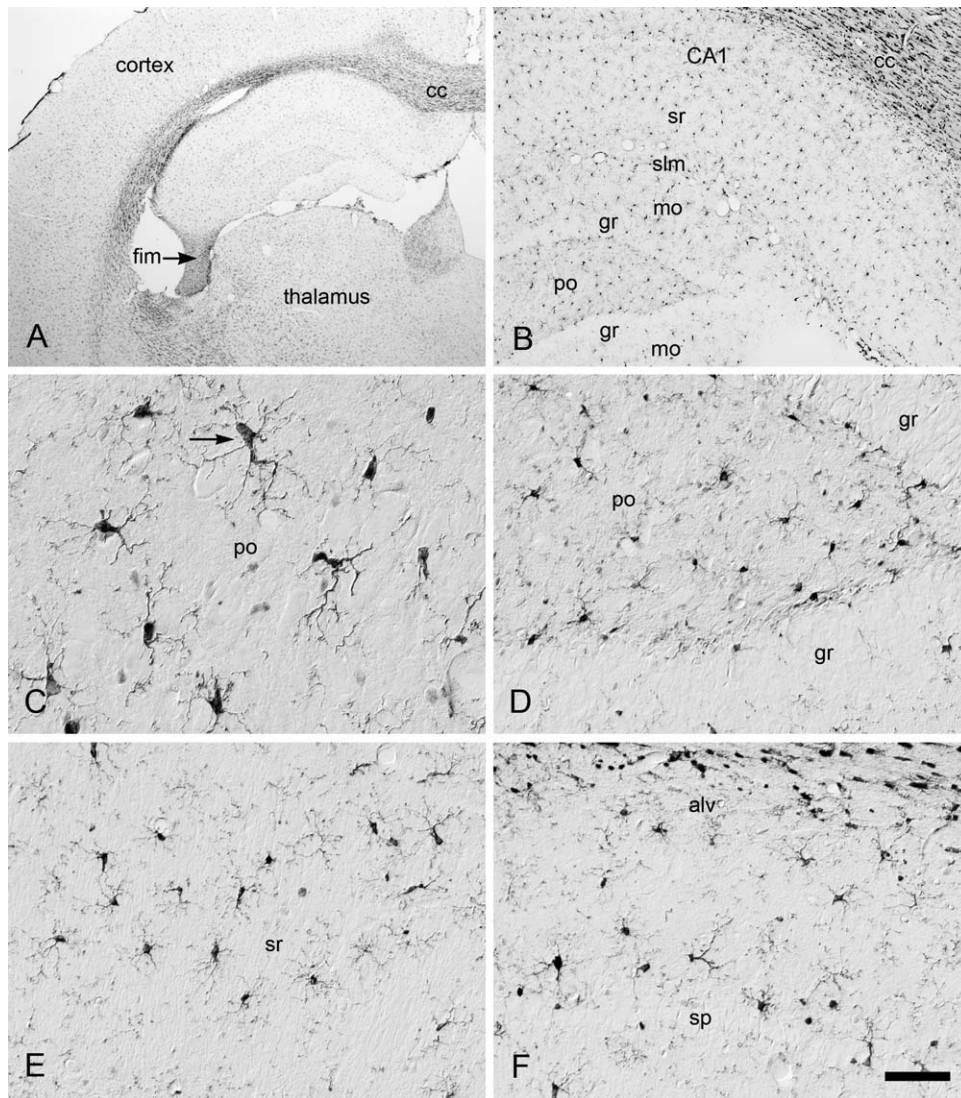


Fig. 7. Hippocampus. ASPA expression in hippocampus was similar to other cortical regions, with fewer immunoreactive oligodendrocytes, and a substantial number of immunoreactive microglia. Microglia were immunoreactive in their cytoplasm and nuclei, but many had stronger staining in their cytoplasm than in their nucleus (C, arrow). ASPA expressing microglia were present in all layers (B–F), with the lowest

density occurring in the granule cell layer (D). alv, alveus; cc, corpus callosum; gr, granule cell layer; mo, molecular layer; po, polymorph layer; slm, stratum lacunosum moleculare; sp, pyramidal cell layer; sr, stratum radiatum. Scale bar = 1 mm A, 300 μ m B, 30 μ m C, and 60 μ m D–F (DIC optics C–F, extended depth of field in panel C).

only lightly stained for ASPA (arrows in Fig. 9C,E), whereas the peripheral portions of the oculomotor nerve expressed ASPA strongly in Schwann cells (asterisks in Fig. 9E). In contrast, the central roots of nerve III were very strongly immunoreactive for MBP (arrows in Fig. 9D,F), but the peripheral portions of the nerve were completely unstained for MBP (asterisks in Fig. 9F) demonstrating the lack of congruence between ASPA and MBP expression.

Cerebellum

The rat cerebellum exhibited a wide range of ASPA expression, with relatively low levels in the cortex, and

very high levels in white matter and deep nuclei (Fig. 10A). In cerebellar cortex, ASPA expression in the molecular layer occurred almost exclusively in ramified microglia (Fig. 10B–D). In contrast, a significant number of stained oligodendrocytes, microglial cells and their associated processes were present in the granule cell layer (Fig. 10B–F). Oligodendrocytes in the granule cell layer had Type I/II morphology, and were interspersed among scattered microglia. In the Purkinje cell layer, strong expression was observed in oligodendrocytes, and faint ASPA expression was observed in cells that may have been Bergmann glial cells, but Purkinje cells were unstained (Fig. 10D). White matter contained numerous strongly stained oligodendrocytes and some immunoreactive microglia (Fig. 10B,C,E,F).

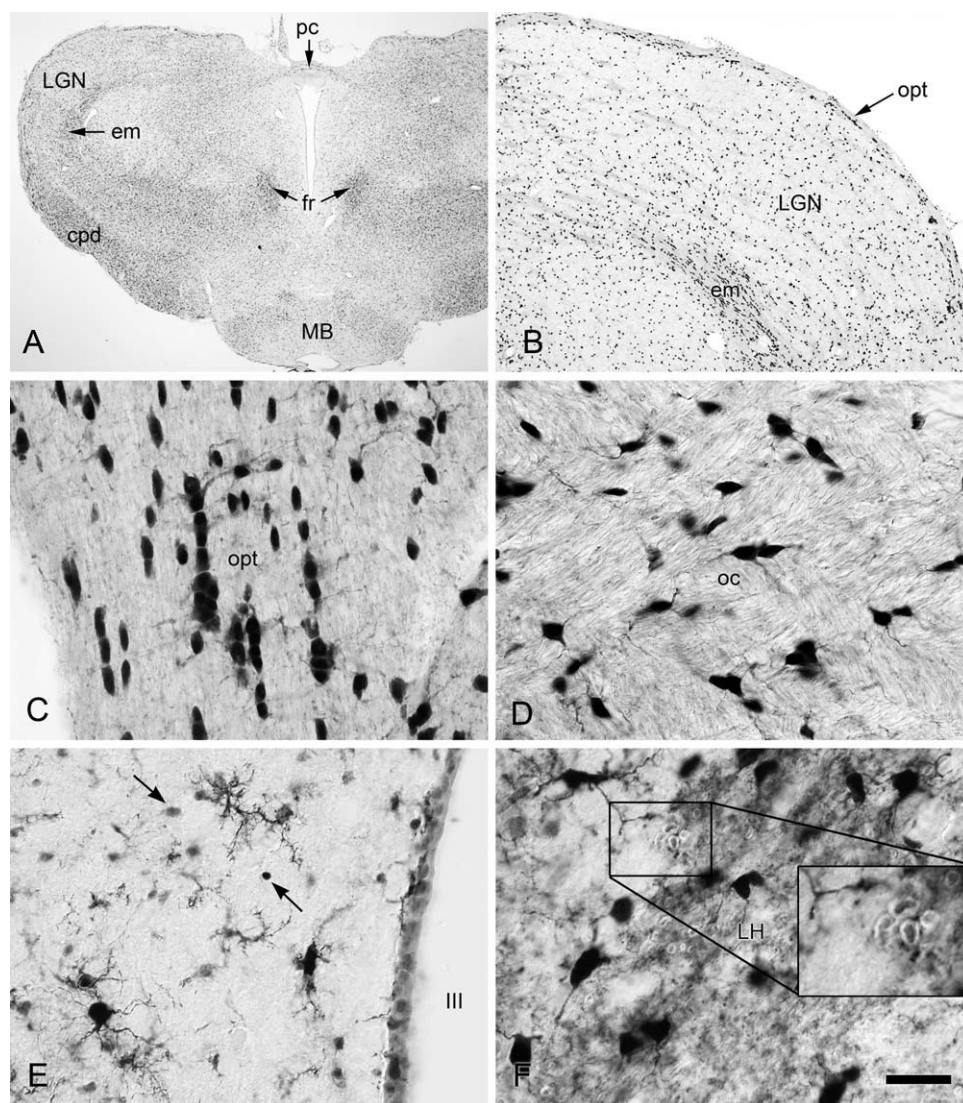


Fig. 8. Thalamus and hypothalamus. ASPA was expressed widely throughout the thalamus, hypothalamus, and mammillary nuclei (A). Fiber pathways such as the optic tracts, fornix, posterior commissure, and external medullary lamina contained numerous ASPA-positive oligodendrocytes (A–D). Gray matter ASPA expression around the third ventricle was predominated by microglia and unidentified cell nuclei (arrows in E). In the lateral hypothalamus, many ASPA-expressing oligodendrocytes were associated with the medial forebrain bundle (F,

antigen retrieval used). At high magnification, the axoplasm of some fibers comprising the medial forebrain bundle was moderately immunoreactive for ASPA, whereas the myelin appeared unstained (inset in F). cpd, cerebral peduncle; em, external medullary lamina; fr, fornix; LGN, lateral geniculate nucleus; LH, lateral hypothalamic area; MB, mammillary bodies; oc, optic chiasm; opt, optic tract; pc, posterior commissure; III, third ventricle. Scale bar = 1 mm A, 300 μ m B, 60 μ m C, 30 μ m D and E, 20 μ m F, and 10 μ m inset in F. (DIC optics B–F).

Brainstem

The brainstem of the rat exhibited some of the strongest ASPA expression in the CNS due to the great density of heavily myelinated fiber tracts (Fig. 11A). Oligodendrocytes with both Type I/II morphology and Type III/IV morphology were observed in the anterior medullary velum at the roof of the fourth ventricle (Fig. 11B). Many of the oligodendrocytes in the brainstem and medulla had a single large process indicative of Type III/IV oligodendrocytes (Fig. 11C–E). In a number of fiber pathways such as the spinal tract of the trigeminal nerve, Type III/IV oligodendrocytes were associated with large diameter axons with unstained myelin sheaths, and ASPA-

positive axoplasm (Fig. 11C, see inset). In cross section these appeared as light toroids (unstained myelin sheaths) with dark centers (stained axoplasm; Fig. 11C,D). Oligodendrocytes with Type III/IV morphology were also observed in other fiber pathways such as the medial cerebellar peduncle and the trapezoid body (Fig. 11D,E). Microglial cells and pial cells also expressed ASPA, as in other parts of the CNS. Choroid plexus epithelial cells within the IV ventricle were unstained. However, the epiplexus cells of the choroid plexus expressed ASPA at moderate levels (Fig. 11F). These ventricular macrophages, also known as Kolmer cells, are adherent to the choroid plexus epithelium and act as ventricular phagocytes.

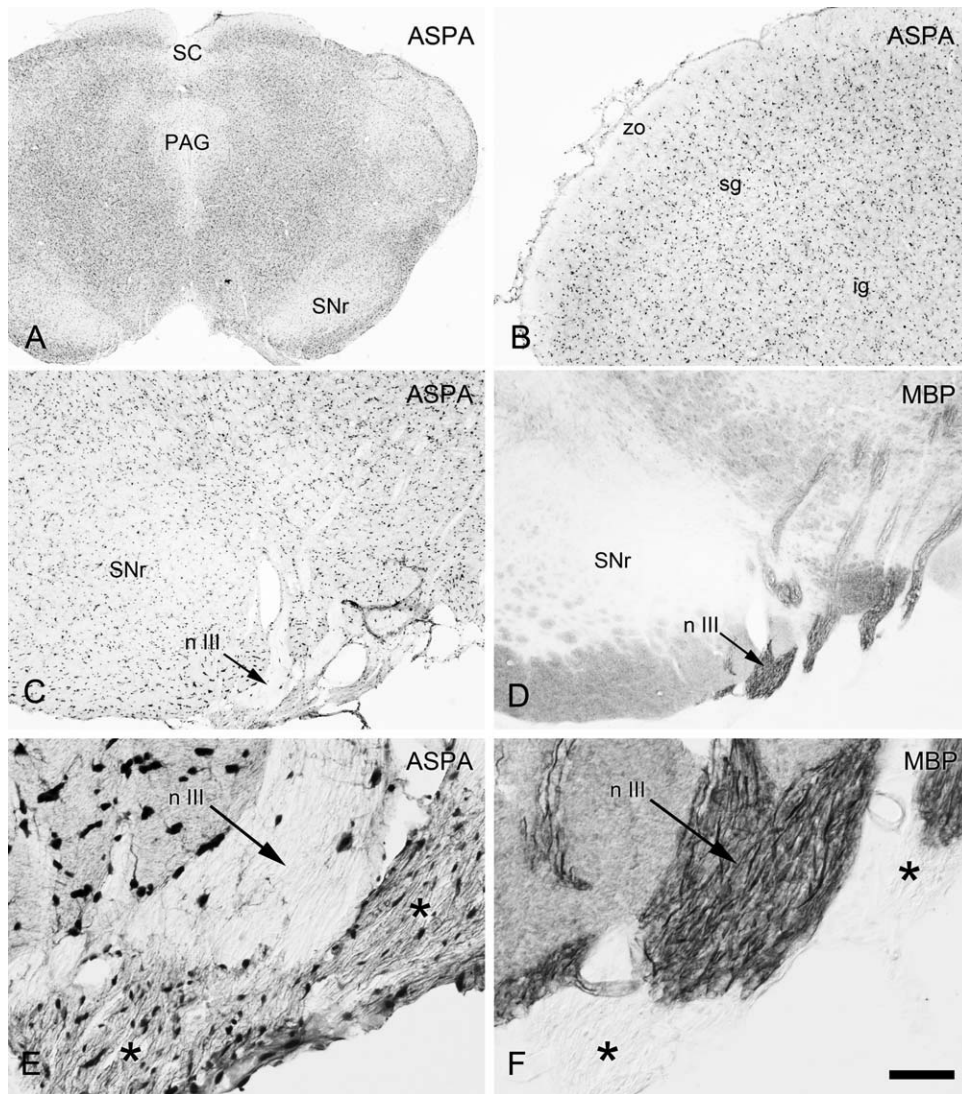


Fig. 9. Midbrain. ASPA expression was relatively low in midbrain gray matter including the superior colliculus (SC), the reticular part of the substantia nigra (SNr), and the periaqueductal gray (PAG) (A). ASPA was expressed at relatively low levels in the outer zonal layer of the superior colliculus (zo), but was expressed in many oligodendrocytes and some microglia in the superficial (sg) and intermediate (ig) gray layers (B). Oculomotor nerve (III) fibers were very lightly immunoreactive for ASPA (arrows in C and E) but were strongly immunoreactive

for myelin basic protein (MBP; arrows in D and F). The peripheral roots of the oculomotor nerve were moderately immunoreactive for ASPA, but were not immunoreactive for myelin basic protein (indicated by asterisks in E and F). ig, intermediate gray of SC; n III, third nerve; PAG, periaqueductal gray; SC, superior colliculus; sg, superficial gray of SC; SNr, reticular substantia nigra; zo, zonal layer of SC. Scale bar = 1 mm A, 300 μ m B–D, 60 μ m E and F (DIC optics E and F).

Medulla

ASPA expression in the medulla was very strong, with a high density of immunoreactive cells in fiber pathways and a lower density of immunoreactive cells in cranial nerve nuclei and the medullary reticular formation (Fig. 12A). Oligodendrocytes in fiber pathways expressed ASPA most strongly, and exhibited both Type I/II and Type III/IV morphology due to the mixed population of large and small diameter nerve fibers. Nuclear groups such as the nucleus of the solitary tract and inferior olive had relatively lower levels of expression, and contained many immunoreactive cell nuclei and microglia (Fig. 12A,B). Oligodendrocytes

and the axons of trigeminal neurons were stained in the spinal tract of the trigeminal nerve (Fig. 12C). The ependymal cells lining the central canal were also lightly to moderately immunoreactive for ASPA (Fig. 12D). Some neurons in the brainstem expressed ASPA at low to moderate levels, for example in the accessory inferior olive and lateral reticular nucleus (Fig. 12E,F). Many of these neurons were not stained any more strongly than their surrounding neuropil, making them difficult to image. Unlike other cell types which showed both cytoplasmic and nuclear staining, ASPA expression in neurons was typically restricted to the cytoplasm, and excluded from their nuclei. Overall, the majority of neuronal cell bodies did not express detect-

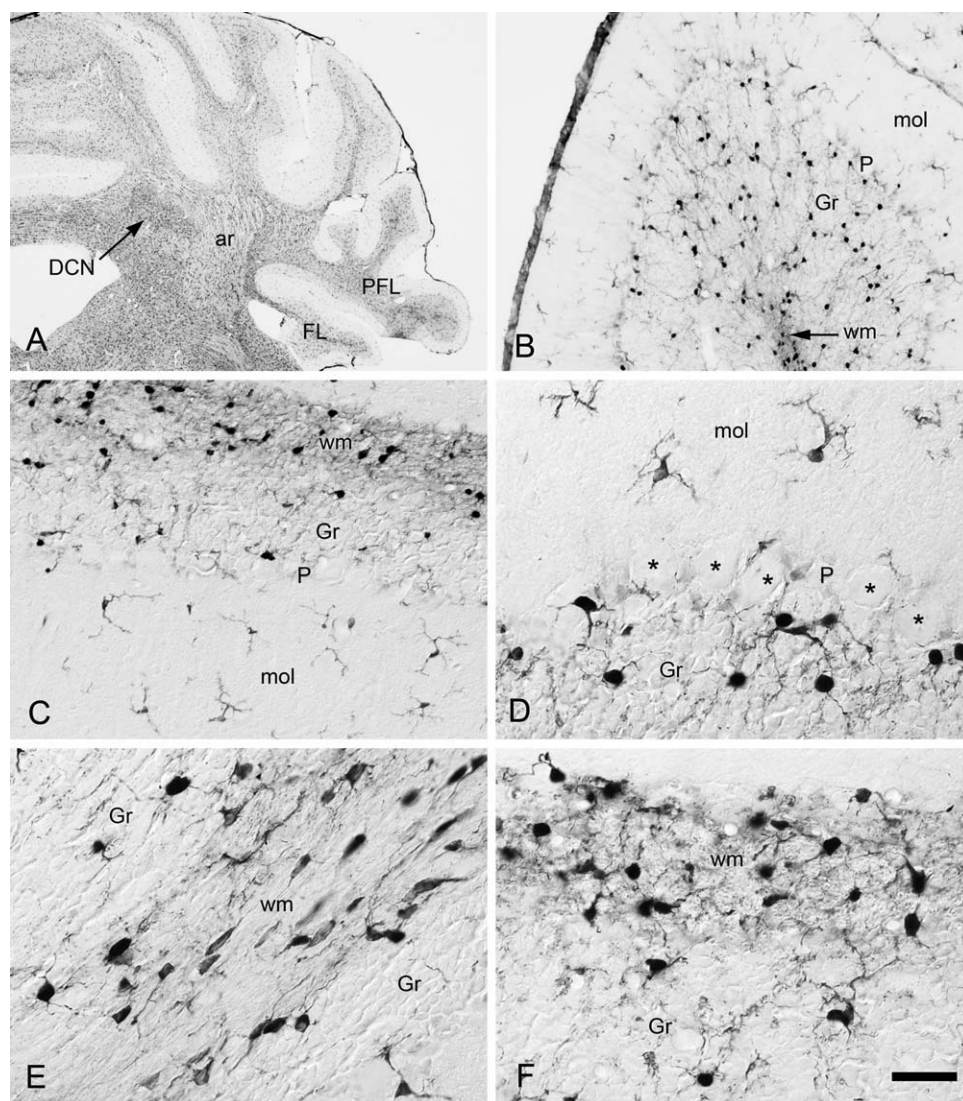


Fig. 10. Cerebellum. ASPA was expressed strongly in the cerebellar white matter (A). In cerebellar, cortex expression was strongest in white matter, and intermediate in the granule and Purkinje cell layers, with the molecular layer having the lowest expression level (B and C). Purkinje cells were unstained (asterisks in D). Immunoreactive oligodendrocytes predominated in white matter and the granule cell layer, whereas microglia were the predominant ASPA expressing cells in the

molecular layer (D). Cerebellar white matter oligodendrocytes are shown sectioned parallel to the neuronal fibers in panel (E) and in cross section in panel (F). ar, arbor vitae; FL, flocculus; Gr, granule cell layer; mol, molecular layer; nVIII, 8th nerve; P, Purkinje cell layer; PFL, paraflocculus; wm, white matter. Scale bar = 1 mm A, 120 μ m B, 60 μ m C, 30 μ m D–F (DIC optics C–F).

able levels of ASPA despite many of the axons originating from those cranial nerve nuclei being moderately stained.

ASPA and AceCS1 Expression in Neuronal Axons

The fiber pathways containing ASPA-expressing axons in the hindbrain also expressed AceCS1 (Fig. 13). This was particularly evident in several cranial nerve pathways, including the spinal tract of the trigeminal nerve, and the seventh and eighth cranial nerves. In the spinal tract of the trigeminal nerve both AceCS1 (Fig. 13A) and ASPA (Fig. 13B) immunoreactivity in axons cut on end had a characteristic toroidal appearance with stained central axoplasm and a surrounding unstained

ring of myelin. In the facial (seventh) nerve, many axons were immunoreactive for both AceCS1 (Fig. 13C) and ASPA (Fig. 13D). AceCS1 was expressed predominantly in the nuclei of oligodendrocytes in the nerve, whereas ASPA was expressed strongly in their nuclei, cytoplasm and some processes. In the eighth nerve, both AceCS1 (Fig. 13E) and ASPA (Fig. 13F) were observed in many axons. Dual labeling immunofluorescence studies will be necessary to determine to what extent both proteins are expressed in the same axons.

Spinal Cord

ASPA expression in the spinal cord was strong in oligodendrocytes, and moderate in some neurons and many

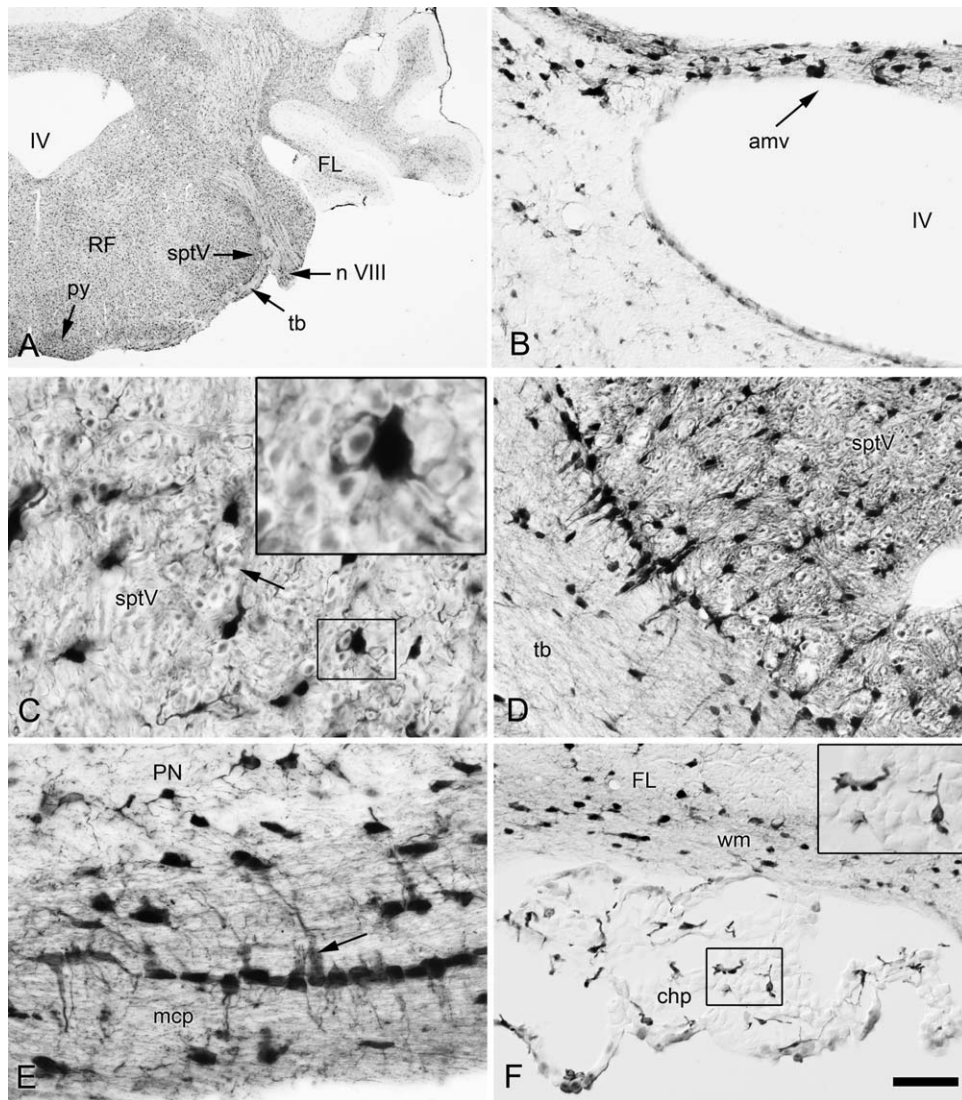


Fig. 11. Brainstem. ASPA expression was very strong in the brainstem due to the density of myelinated axons (A). Oligodendrocytes in the anterior medullary vellum strongly expressed ASPA (B; amv). In some fiber pathways cut in cross section, myelin sheaths appeared completely unstained, whereas the axoplasm in different nerve fibers ranged from unstained to moderately stained for ASPA (C, arrow and inset and D). In many hindbrain fiber pathways, some oligodendrocytes issued one major process that coursed perpendicular to the orientation of axons in the fiber pathway,

including the trapezoid body (D; tb) and middle cerebellar peduncle (E; mcp, see arrow). Moderate to strong ASPA expression was present in Kolmer (epi-plexus) cells associated with the choroid epithelium (F; inset = enlargement of boxed area). amv, anterior medullary vellum; chp, choroid plexus; FL, flocculus; IV, 4th ventricle; mcp, middle cerebellar peduncle; n VIII, 8th nerve; PN, pontine gray; py, pyramids; RF, reticular formation; sptV, spinal tract of the trigeminal nerve; tb, trapezoid body. Scale bar = 1 mm A, 30 μ m C, E and inset in F, 60 μ m B, D and F, 15 μ m inset in C (DIC optics B-F).

axons (Fig. 14A). Strong expression was observed in the dorsal columns, with the pyramidal tracts and cuneate fasciculi having the highest immunoreactivity (Fig. 14A,B). More neuronal cell bodies expressed ASPA in the spinal cord gray matter than any other region of the CNS (Fig. 14C,D). The most immunoreactive neurons were motor neurons of Layer 9 (Fig. 14D). Axonal fibers of the pyramidal tracts (Fig. 14A,B) and the axons of the cuneate and gracile funiculi were immunoreactive seen cut on end, whereas myelin sheaths appeared unstained (Fig. 14E,F). Many axonal fibers in the lateral and ventral funiculi were also immunoreactive.

DISCUSSION

Confirming and expanding upon our earlier findings with a different anti-ASPA antibody (Madhavarao et al., 2004) we found that most cell types in the brain can express ASPA indicating a broader functional repertoire for NAA, and NAA-derived acetate and aspartate, than previously recognized. All ASPA-immunoreactive elements observed in wild type rat brain sections were absent in brain sections from tremor rats, a mutant rat strain which lacks the entire ASPA gene sequence. The previous ASPA antibody used in our laboratory was produced against purified full-length recombinant ASPA

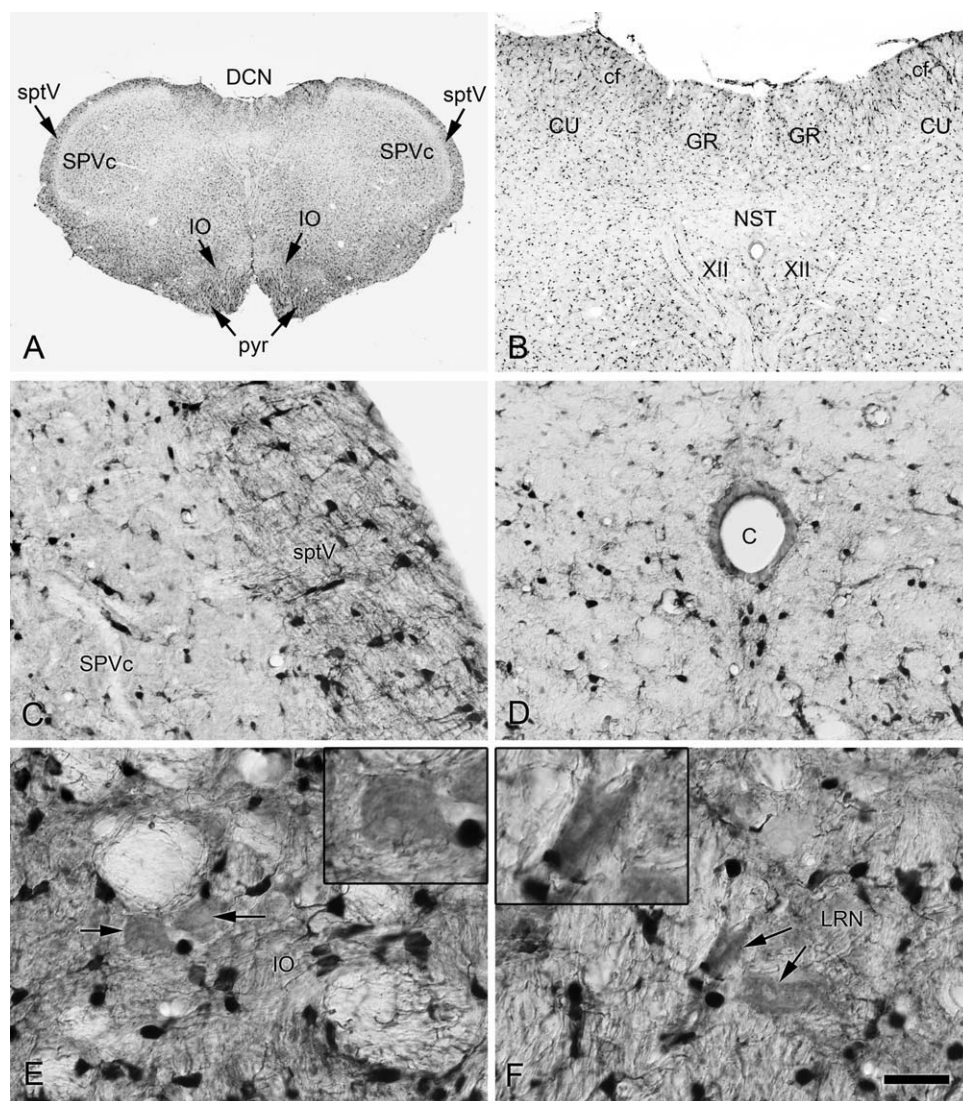


Fig. 12. Medulla. ASPA was expressed extensively throughout the medulla (A). Oligodendrocytes in fiber pathways expressed ASPA strongly, for example in the pyramids, spinal tract of the trigeminal nerve (sptV), and the dorsal column pathways including the cuneate fasciculus (B). Oligodendrocytes and neuronal axons were stained in the spinal tract of the trigeminal nerve (C). Ependymal cells lining the central canal were moderately immunoreactive for ASPA (D). A relatively small number of neurons with large cell bodies expressed ASPA at low to

moderate levels, for example in the inferior olive and lateral reticular nucleus (arrows and insets in panels E and F). c, central canal; cf, cuneate fasciculus; CU, cuneate nucleus; GR, gracile nucleus; DCN, dorsal column nuclei; IO, inferior olive (accessory); LRN, lateral reticular nucleus; NST, nucleus of the solitary tract; pyr, pyramids; sptV, spinal tract of the trigeminal nerve; SPVc, spinal nucleus of the trigeminal nerve (caudal); XII, hypoglossal nucleus. Scale bar = 1 mm A, 300 μ m B, 60 μ m C and D, 30 μ m E and F, 15 μ m insets (DIC optics C-F).

protein. That antibody and the one used in the current study both stained the same cellular elements. Astrocytes were the only major cell type in the brain that did not express ASPA in their cytoplasm at detectable levels with either antibody.

ASPA Expression in Oligodendrocytes

ASPA expression was observed extensively in oligodendrocytes throughout the CNS, with virtually all oligodendrocytes showing some level of ASPA expression. ASPA immunoreactivity in oligodendrocytes was often uniformly strong in both the cytoplasm and nucleus, but

in some the staining was stronger in one subcellular compartment or the other. This finding supports previous results showing that ASPA is transported between cytoplasmic and nuclear compartments (Hershfield et al., 2006). ASPA was also expressed in some oligodendrocyte processes, but was absent in many processes and in compact myelin. However, ASPA was expressed immediately adjacent to myelin sheaths in terminal oligodendrocyte processes and possibly in paranodal oligodendrocyte cytoplasm.

Oligodendrocytes are the macroglial cells responsible for producing myelin sheaths in the CNS, and they employ bidirectional trophic and metabolite exchanges with neuronal axons to accomplish this highly special-

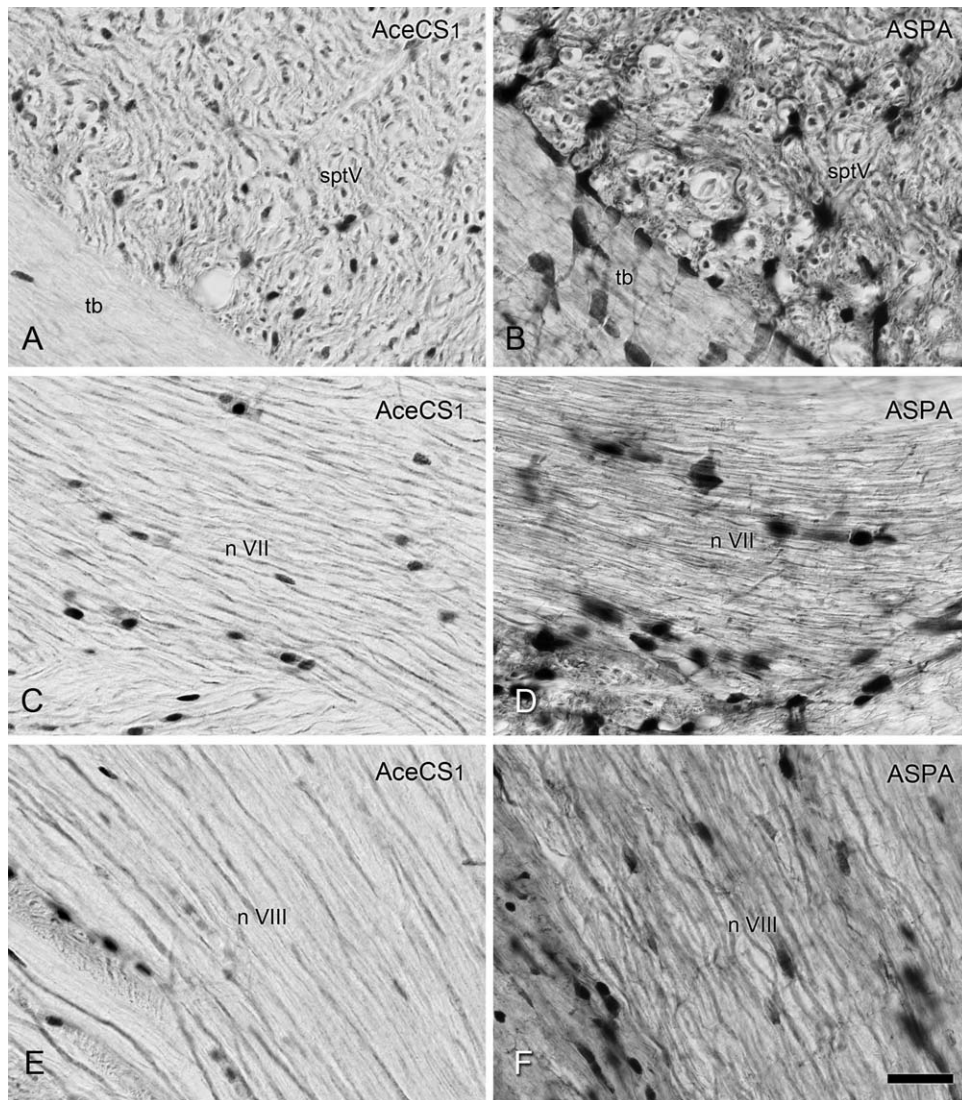


Fig. 13. AceCS1 and ASPA immunoreactivities in axons from several cranial nerves. AceCS1 (A, C, and E) and ASPA (B, D, and F) were moderately expressed in the axoplasm of many of the axonal fibers in several cranial nerves, including the fifth, seventh, and eighth nerves. In addition, oligodendrocytes were immunoreactive for ASPA in

their nuclei, cytoplasm, and some processes, but AceCS1 was present predominantly in oligodendrocyte nuclei. n VII, 7th cranial nerve; n VIII, 8th cranial nerve; sptV, spinal tract of the trigeminal nerve; tb, trapezoid body. Scale bar = 30 μ m (DIC optics A–F).

ized cellular behavior (Ledeen, 1984; Nave, 2010; Popko, 2003). NAA is one of these trophic molecules supplied by neurons, and NAA-derived acetate contributes to myelin lipid synthesis in oligodendrocytes during postnatal development (reviewed in Moffett et al., 2007). The contribution of NAA derived acetate to myelination is most critical during the period of postnatal myelination, at which time it constitutes ~30% of the carbon incorporated into certain myelin associated lipids including cerebroside (Madhavarao et al., 2005; Traka et al., 2008; Wang et al., 2009). The bulk of acetyl CoA utilized to synthesize myelin lipids comes from citrate synthesized in oligodendrocyte mitochondria. Citrate is produced in mitochondria from pyruvate in the TCA cycle and is then exported to the cytoplasm. The enzyme ATP citrate lyase converts cytosolic citrate into acetyl CoA, which

then is used to synthesize the fatty acids and sterols needed for myelination. The NAA-derived acetate produced in oligodendrocytes through the action of ASPA can not be used for lipid synthesis until it is converted to acetyl CoA. This is accomplished by acetyl coenzyme A synthase-1 (AceCS1), which is present in many oligodendrocytes during postnatal myelination (Ariyannur et al., 2010a). AceCS1 catalyzes the reaction between free acetate and coenzyme A to produce acetyl CoA, which then can participate in cellular metabolism. Therefore, there are two parallel pathways of acetyl CoA generation in oligodendrocytes for lipid synthesis during myelination, the primary citrate/ATP citrate lyase pathway and the secondary NAA/ASPA-AceCS1 pathway (Ariyannur et al., 2010a; Arun et al., 2010; Moffett et al., 2007).

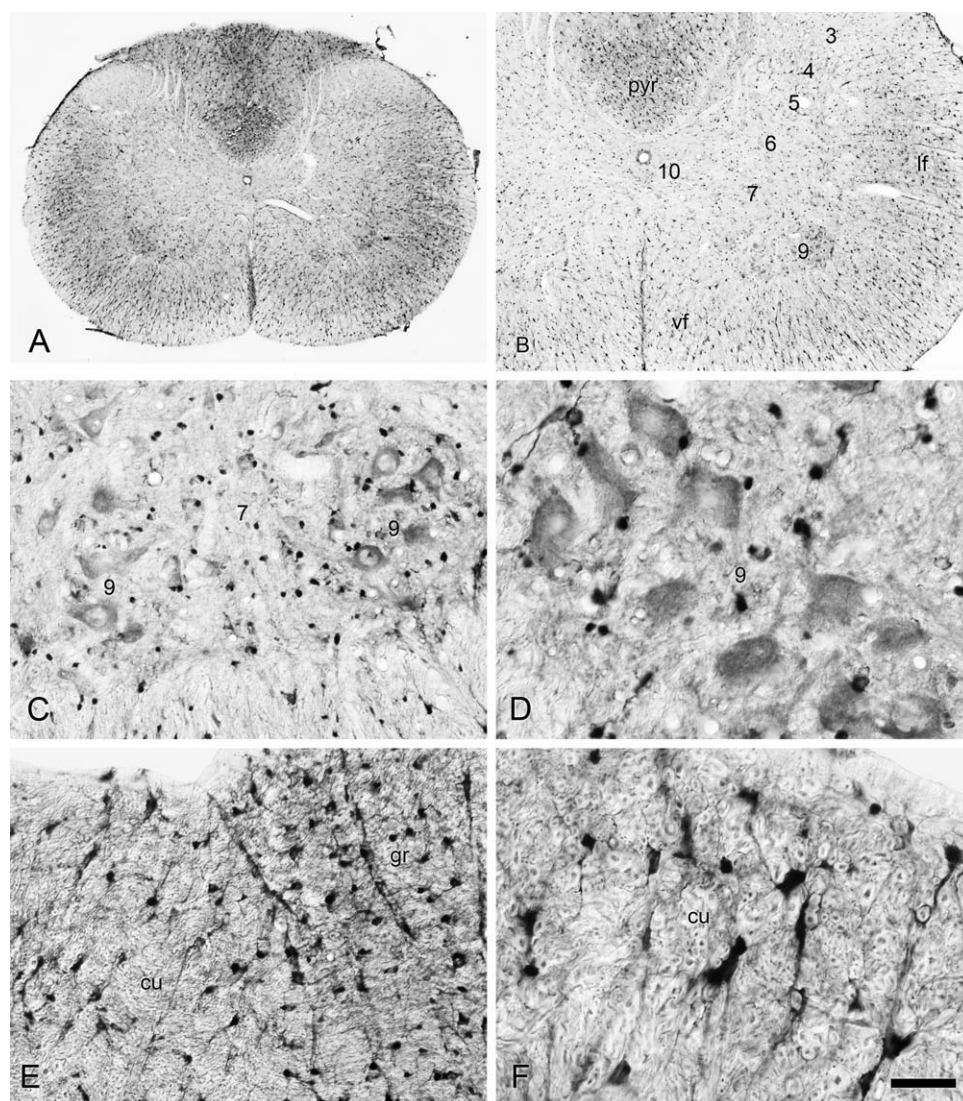


Fig. 14. Spinal cord. ASPA was expressed strongly in the rat spinal cord, with the dorsal columns exhibiting particularly intense staining (A). Gray matter staining was generally lower than staining in fiber tracts (B). Layer 9 motor neurons of the ventral horn were lightly to moderately immunoreactive for ASPA, with most expression in the cytoplasm (C and D). The dorsal columns contained numerous ASPA

positive oligodendrocytes (E), and many axons cut in cross section showed ASPA immunoreactivity in the axoplasm, but not myelin (F). 3-7, 9, and 10, layers of spinal gray matter; cu, cuneate fasciculus; gr, gracile fasciculus; lf, lateral funiculus; pyr, pyramidal tracts; vf, ventral funiculus. Scale bar = 300 μ m A, 200 μ m B, 60 μ m C and E, and 30 μ m D and F (DIC optics C-F).

ASPA has been reported to be present in the brain primarily as a soluble enzyme in the cytosol fraction (D'Adamo et al., 1973, 1977; Klugmann et al., 2003; Madhavarao et al., 2004). However, other studies have provided evidence that some proportion of brain ASPA is associated with myelin (Chakraborty et al., 2001; Wang et al., 2007), and that detergent is required to dissociate this fraction of enzyme activity from membranes or myelin (Goldstein, 1976; Wang et al., 2007). In the current study, ASPA expression in white matter was observed in some oligodendrocyte processes associated with neuronal axons that could represent localization within myelin sheaths, or the cytoplasmic layers associated with myelin. However, the staining patterns for ASPA and two myelin associated proteins, MBP and OSP, were not

similar at low or high magnification (Figs. 3, 4, and 9). At higher magnification, ASPA immunoreactivity in major caudal fiber pathways was clearly present in the axoplasm of many axons cut on end, but was not observed in the ensheathing myelin (Figs. 8, 11, and 14). In contrast, MBP and OSP were associated with myelin sheaths and oligodendrocyte processes respectively.

ASPA Expression in Microglia and Meninges

Microglia expressed ASPA throughout the CNS and were more apparent in cortical and gray matter areas than in fiber pathways. Previously we reported that some microglia were lightly to moderately immunoreac-

tive for ASPA in the rat CNS using a different ASPA antibody (Madhavarao et al., 2004). In the current study utilizing purified ASPA peptide antibodies we observed that microglia were immunoreactive throughout the CNS, and ranged from lightly to strongly immunoreactive. All ASPA expressing microglia were highly ramified in morphology indicating that they were in a resting, non-immunogenic state. Microglia are related to macrophages (Guillemin et al., 2004; Streit et al., 1993), and we observed that macrophages associated with the choroid plexus, so-called epiplexus cells (Ling et al., 1998) also expressed ASPA moderately (Fig. 11F). ASPA expressing microglia were also observed in the subfornical organ (Fig. 6A, inset), a circumventricular organ whose cells lie outside the blood brain barrier. These findings suggest that ASPA expression may be common among phagocytic cells, and in fact, we have observed strong ASPA expression in apparent macrophages throughout the rat spleen (unpublished observations). Recently, the *N*-acetyltransferase-8-like gene has been shown to be the gene encoding the NAA synthesizing enzyme aspartate *N*-acetyltransferase (Ariyannur et al., 2010b; Wiame et al., 2010). This gene was found to be expressed in only 3 of the tissues examined; brain, and to lesser extents in spleen and thymus (Wiame et al., 2010). This is consistent with some immune cell types being capable of synthesizing NAA.

Leptomeningeal cells of the pia mater expressed ASPA very strongly, and some endothelial cells of the cerebral vasculature expressed low levels of ASPA. Ependymal cells also expressed ASPA at low to moderate levels. It is possible that ASPA expression in the meninges, ependymal cells and vasculature could provide a mechanism for scavenging NAA from the cerebral circulation and cerebrospinal fluid allowing uptake of the resultant aspartate and acetate for recycling to the brain. This possibility is consistent with observation that NAA levels drop as cerebrospinal fluid passes from ventricles (~55 μ M) to the subarachnoid space (~9 μ M) and then to lumbar spinal cord (~1 μ M) (Faull et al., 1999). Retention of the resultant metabolites would be more critical under low nutrient conditions, or at times of high metabolic demand.

ASPA and ACS1 Expression in Cell Nuclei

In every region of the CNS examined the nuclei of oligodendrocytes, microglial cells, endothelial cells, ependymal cells, epiplexus cells and leptomeningeal cells, as well as numerous unidentified cell nuclei, were immunoreactive for ASPA. This finding is highly relevant to the recently described localization of AceCS1, which was found to be localized predominantly to cell nuclei in the adult rat brain (Ariyannur et al., 2010a). As noted above, AceCS1 is present in the cytoplasm and nuclei of oligodendrocytes during postnatal myelination, but the expression pattern shifts to a predominantly nuclear localization in adult rats (Ariyannur et al., 2010a). AceCS1 was also expressed in the nuclei of neurons and astrocytes, as well as in many unidentified cell nuclei in

all regions of the CNS. There are only two known forms of acetyl coenzyme A synthase, types 1 and 2, with Type II being localized to mitochondria where it synthesizes acetyl CoA for energy derivation (Fujino et al., 2001; Sakakibara et al., 2009). As such, AceCS1 is the only known enzyme capable of converting free acetate into acetyl CoA in cell nuclei, where AceCS1 may be acting to recycle acetate derived from deacetylation reactions such as histone deacetylase activity. In addition to AceCS1 acting to recycle acetate derived from deacetylase reactions, mounting evidence supports a role for NAA and nuclear localized ASPA in providing some of the acetate for protein acetylation reactions including histone acetylation. In such a scenario, NAA present in the nucleus is broken down by nuclear-localized ASPA, and the free acetate is then converted to acetyl CoA by the action of AceCS1. The acetyl CoA produced can then be utilized by histone acetyltransferase enzymes for nuclear histone acetylation reactions involved in chromatin remodeling and epigenetic gene regulation. Recently we found that AceCS1 expression in oligodendrocyte and neuronal cell nuclei is increased in the tremor rat model of Canavan disease, and that chronic treatment with a hydrophobic acetate precursor normalizes AceCS1 expression levels in this model, suggesting that the lack of NAA-derived acetate leads to altered acetyl CoA metabolism in the CNS (Ariyannur et al., 2010b; Arun et al., 2010). The important role of epigenetic gene regulation in oligodendrocyte maturation has been reviewed recently (Coprav et al., 2009; Liu et al., 2010).

In single celled eukaryotes such as yeast AceCS1 is a primary source of acetyl CoA required for histone acetylation reactions and gene transcription (Takahashi et al., 2006). In contrast, mammalian cells derive most of their acetyl CoA for histone acetylation reactions via the ATP citrate lyase pathway (Wellen et al., 2009). This is analogous to the roles of these two enzyme systems in mammalian lipid synthesis. Therefore in mammals both lipid synthesis and histone acetylation derive most of their acetyl CoA from glucose (pyruvate) by way of citrate and ATP citrate lyase. The role of AceCS1 in histone acetylation in mammals appears to be a secondary, parallel pathway for acetyl CoA production.

ASPA Expression in Neurons and their Axons

In the current study, we confirm our previous finding that ASPA is expressed in a substantial number of axons in the rodent brain. In a previous study using a different anti-ASPA antibody, we observed mild to moderate ASPA-immunoreactivity in some large neurons in the brainstem and spinal cord, as well as in numerous axons in certain fiber tracts (Madhavarao et al., 2004). In that study, we did not have access to tremor rat tissue, and therefore could not definitively confirm that all immunoreactivity was due to ASPA protein expression. In the present study using the purified ASPA peptide antibody, some neurons were found to express ASPA protein in their perikarya (Figs. 12E,F and 14C,D), but tremor rat

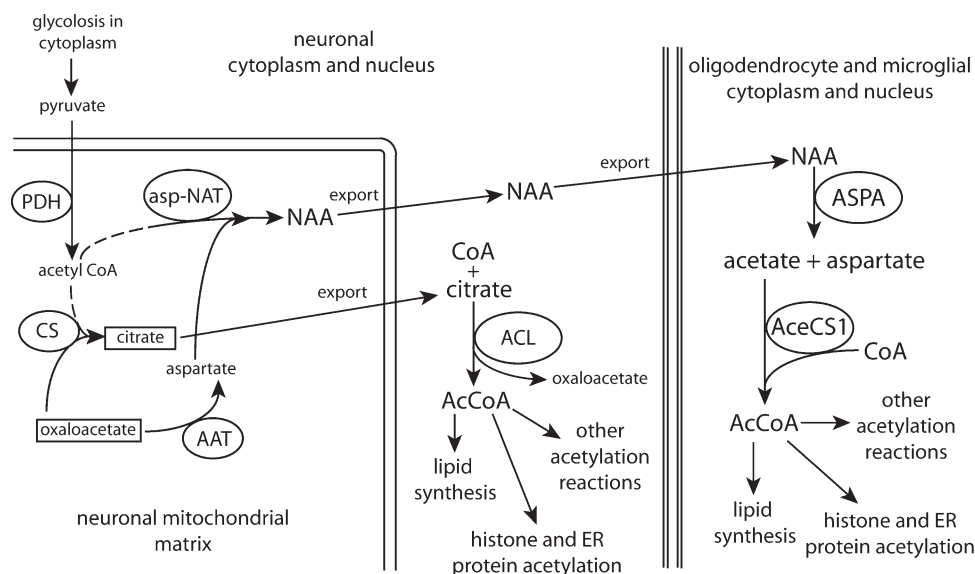


Fig. 15. Schematic diagram of the metabolic similarity between citrate and NAA. Citrate and NAA are synthesized from acetyl CoA in neuronal mitochondria. Citrate synthesis requires oxaloacetate, whereas NAA synthesis requires aspartate. Both citrate and NAA are exported from mitochondria to the cytoplasm. Citrate and coenzyme A are converted in the neuronal cytoplasm into acetyl CoA and oxaloacetate, and the acetyl CoA can then be used for all acetylation reactions in the cytoplasm and nucleus.

NAA, unlike citrate, can be targeted to other cell types, including oligodendrocytes and microglia. After transport to glial cells, the NAA is converted to acetate and aspartate by ASPA, and the acetate plus coenzyme A are then converted to acetyl CoA by AceCS1. AAT, aspartate aminotransferase; AceCS1, acetyl coenzyme A synthase-1; ACL, ATP citrate lyase; ASPA, aspartoacylase; asp-NAT, aspartate *N*-acetyltransferase; CS, citrate synthase; ER, endoplasmic reticulum; PDH, pyruvate dehydrogenase.

brain sections showed no immunoreactivity, indicating that the neuronal staining in wild type rats was specific for ASPA. Most neurons did not express detectable ASPA levels in their cytoplasm, but many did express ASPA in their axoplasm, and this was especially apparent in long axonal projections comprised of medium to large diameter fibers, such that they were associated with Type III/IV oligodendrocytes. The lack of ASPA expression in most neuronal cell bodies with concomitant expression in their axons is suggestive of rapid transport of newly synthesized ASPA protein from perikarya to axons.

Previously, it has been assumed that the synthetic and degradative compartments for NAA were invariably located in distinct cell types wherein neurons synthesize NAA, and subsequently transfer it to oligodendrocytes for catabolism (Baslow, 2003, 2010; Baslow et al., 1999). Based on the current findings that ASPA is expressed in axons, this assumption must be reexamined. Many of the fiber pathways found to express ASPA in the current study have also been reported to contain both NAA, and the related neuronal dipeptide *N*-acetyl-aspartylglutamate (NAAG) (Moffett et al., 1993, 2006). The observation that a substantial number of axons express low to moderate levels of ASPA indicates that NAA can be both synthesized and degraded in a single cell type within the CNS. A number of caudal fiber tracts such as the spinal tract of the trigeminal nerve, the spinocerebellar tract, several cranial nerves, the pyramidal tracts and the dorsal columns were moderately immunoreactive for ASPA in their axoplasm. The expression of ASPA in the axons of projection pathways and nerves exhibited a generally increasing gradient of expression

from forebrain to hindbrain, but this may have been due in part to the diameter of axons in forebrain and hindbrain. It was difficult to image individual axons in forebrain fiber pathways due to their smaller diameter, but the axoplasm of fibers in the medial forebrain bundle in the lateral hypothalamus were immunoreactive for ASPA (Fig. 8F). In the current study we also observed AceCS1 expression in many of the same axonal pathways (Fig. 13) suggesting that NAA-derived acetate can be converted to acetyl CoA for further metabolism in some axons. However, determining the extent of ASPA and AceCS1 colocalization in axons will require future dual labeling immunofluorescence studies.

Existing evidence indicates that NAA is synthesized primarily in neurons from acetyl CoA and aspartate and that a substantial portion is stored in neurons, whereas some is exported to other cell types including oligodendrocytes. It is likely that NAA is synthesized in neurons when acetyl CoA is produced in excess of local requirements, for example when glucose levels are high. The acetyl CoA is converted to NAA in neurons and is stored for later use. It is possible that the low synthesis rate reported for NAA under resting conditions (Harris et al., 2006) is a reflection of this storage role. As metabolic demands outweigh local glucose and pyruvate supplies, some of the stored NAA is broken down by ASPA in order to regenerate acetyl CoA, either in the axon of same neuron or more generally, in cells in contact with the neuron after intercellular NAA transport. Virtually all cell types in the brain are in direct contact with neurons including oligodendrocytes, astrocytes and microglia (Peters et al., 1991), and are therefore in a position to receive intercellularly transported NAA directly via

cell contacts. When neuronal activity is high, NAA is transferred to neighboring cells, especially oligodendrocytes, in order to support increased metabolic and physiological demands. NAA may therefore be acting as a storage and transport form of acetyl CoA (and aspartate) critical for proper nervous system development and function (Ariyannur et al., 2010b; Arun et al., 2010). Because acetyl CoA participates in so many diverse cellular functions, NAA may also participate in the same functions by delivering acetate (as well as aspartate) to the many cell types in the brain that express ASPA.

One way in which NAA could support brain metabolism when neural activity levels were high would be to substitute for cytoplasmic citrate in cells that express both ASPA and AceCS1 (Fig. 15). Each molecule of acetyl CoA produced from NAA-derived acetate means one less citrate molecule must be exported from local mitochondria. As such, pre-existing intramitochondrial acetyl CoA is spared from being converted to citrate, and instead can be used to generate energy via the TCA cycle. NAA delivery to the cytoplasm (and nuclei) of oligodendrocytes, microglia and other cell types means that their mitochondria can use their current acetyl CoA complement for oxidative phosphorylation, rather than to synthesize and export citrate. NAA can substitute by providing both acetyl CoA and oxaloacetate (via aspartate) in the cytoplasm, as would be the case when ATP citrate lyase breaks down citrate into acetyl CoA and oxaloacetate. These emerging views on functional roles of ASPA suggest a much more complicated picture than previously recognized.

REFERENCES

- Adachi M, Schneck L, Cara J, Volk BW. 1973. Spongy degeneration of the central nervous system (van Bogaert and Bertrand type; Canavan's disease). A review. *Hum Pathol* 4:331–347.
- Alving RE, Laki K. 1966. N-terminal sequence of actin. *Biochemistry* 5:2597–2601.
- Ariyannur PS, Moffett JR, Madhavarao CN, Arun P, Vishnu N, Jacobowitz D, Hallows WC, Denu JM, Nambodiri AM. 2010a. Nuclear-cytoplasmic localization of acetyl coenzyme A synthetase-1 in the rat brain. *J Comp Neurol* 518:2952–2977.
- Ariyannur PS, Moffett JR, Manickam P, Pattabiraman N, Arun P, Nitta A, Nabeshima T, Madhavarao CN, Nambodiri AM. 2010b. Methamphetamine-induced neuronal protein NAT8L is the NAA biosynthetic enzyme: Implications for specialized acetyl coenzyme A metabolism in the CNS. *Brain Res* 1335:1–13.
- Arun P, Madhavarao CN, Moffett JR, Hamilton K, Grunberg NE, Ariyannur PS, Gahl WA, Anikster Y, Mog S, Hallows WC, Denu JM, Nambodiri AM. 2010. Metabolic acetate therapy improves phenotype in the tremor rat model of Canavan disease. *J Inherit Metab Dis* 33:195–210.
- Baslow MH. 2003. N-acetylaspartate in the vertebrate brain: Metabolism and function. *Neurochem Res* 28:941–953.
- Baslow MH. 2010. Evidence that the tri-cellular metabolism of N-acetylaspartate functions as the brain's "operating system": How NAA metabolism supports meaningful intercellular frequency-encoded communications. *Amino Acids* 39:1139–1145.
- Baslow MH, Suckow RF, Sapirstein V, Hungund BL. 1999. Expression of aspartoacylase activity in cultured rat macroglial cells is limited to oligodendrocytes. *J Mol Neurosci* 13:47–53.
- Birnbaum SM. 1955. Amino acid acylases I and II from hog kidney. *Methods Enzymol* 2:115–119.
- Burri R, Steffen C, Herschkowitz N. 1991. N-acetyl-L-aspartate is a major source of acetyl groups for lipid synthesis during rat brain development. *Dev Neurosci* 13:403–412.
- Butt AM, Ibrahim M, Berry M. 1998. Axon-myelin sheath relations of oligodendrocyte unit phenotypes in the adult rat anterior medullary velum. *J Neurocytol* 27:259–269.
- Chakraborty G, Mekala P, Yahya D, Wu G, Ledeen RW. 2001. Intra-neuronal N-acetylaspartate supplies acetyl groups for myelin lipid synthesis: evidence for myelin-associated aspartoacylase. *J Neurochem* 78:736–745.
- Copray S, Huynh JL, Sher F, Casaccia-Bonnel P, Boddeke E. 2009. Epigenetic mechanisms facilitating oligodendrocyte development, maturation, and aging. *Glia* 57:1579–1587.
- D'Adamo AF, Gidez LI, Yatsu FM. 1968. Acetyl transport mechanisms. Involvement of N-acetyl aspartic acid in de novo fatty acid biosynthesis in the developing rat brain. *Exp Brain Res* 5:267–273.
- D'Adamo AF Jr, Peisach J, Manner G, Weiler CT. 1977. N-acetyl-aspartate amidohydrolase: Purification and properties. *J Neurochem* 28:739–744.
- D'Adamo AF Jr, Smith JC, Woiler C. 1973. The occurrence of N-acetylaspartate amidohydrolase (aminoacylase II) in the developing rat. *J Neurochem* 20:1275–1278.
- D'Adamo AF Jr, Yatsu FM. 1966. Acetate metabolism in the nervous system. N-acetyl-L-aspartic acid and the biosynthesis of brain lipids. *J Neurochem* 13:961–965.
- Faulk KF, Raffie R, Pascoe N, Marsh L, Pfefferbaum A. 1999. N-acetylaspartic acid (NAA) and N-acetylaspartylglutamic acid (NAAG) in human ventricular, subarachnoid, and lumbar cerebrospinal fluid. *Neurochem Res* 24:1249–1261.
- Fujino T, Kondo J, Ishikawa M, Morikawa K, Yamamoto TT. 2001. Acetyl-CoA synthetase 2, a mitochondrial matrix enzyme involved in the oxidation of acetate. *J Biol Chem* 276:11420–11426.
- Gaetjens E, Barany M. 1966. N-acetylaspartic acid in G-actin. *Biochim Biophys Acta* 117:176–183.
- Goldstein FB. 1976. Amidohydrolases of brain; enzymatic hydrolysis of N-acetyl-L-aspartate and other N-acyl-L-amino acids. *J Neurochem* 26:45–49.
- Guillemin GJ, Brew BJ. 2004. Microglia, macrophages, perivascular macrophages, and pericytes: A review of function and identification. *J Leukoc Biol* 75:388–397.
- Hagenfeldt L, Bollgren I, Venizelos N. 1987. N-acetylaspartic aciduria due to aspartoacylase deficiency—A new aetiology of childhood leukodystrophy. *J Inherit Metab Dis* 10:135–141.
- Harris K, Lin A, Bhattacharya P, Tran T, Wong W, Ross BD. 2006. Regulation of NAA-synthesis in the human brain *in vivo*: Canavan's disease, Alzheimer's disease and schizophrenia. In: Moffett JR, Tieman SB, Weinberger DR, Coyle JT, Nambodiri MA, editors. *N-Acetylaspartate: A unique neuronal molecule in the central nervous system*. New York, NY: Springer Science + Business Media. pp 263–273.
- Hershfield J, Madhavarao CN, Moffett JR, Benjamins JA, Garbern JY, Nambodiri MA. 2006. Aspartoacylase is a regulated nuclear-cytoplasmic enzyme. *FASEB J* 20:2139–2141.
- Inglese M, Rusinek H, George IC, Babb JS, Grossman RI, Gonen O. 2008. Global average gray and white matter N-acetylaspartate concentration in the human brain. *Neuroimage* 41:270–276.
- Jacobowitz DM. 1974. Removal of discrete fresh regions of the rat brain. *Brain Res* 80:111–115.
- Jakobs C, ten Brink HJ, Langelaar SA, Zee T, Stellaard F, Macek M, Srsnova K, Srsen S, Kleijer WJ. 1991. Stable isotope dilution analysis of N-acetylaspartic acid in CSF, blood, urine and amniotic fluid: Accurate postnatal diagnosis and the potential for prenatal diagnosis of Canavan disease. *J Inherit Metab Dis* 14:653–660.
- Kaul R, Casanova J, Johnson AB, Tang P, Matalon R. 1991. Purification, characterization, and localization of aspartoacylase from bovine brain. *J Neurochem* 56:129–135.
- Kaul R, Gao GP, Balamurugan K, Matalon R. 1993. Cloning of the human aspartoacylase cDNA and a common missense mutation in Canavan disease. *Nat Genet* 5:118–123.
- Kelley RI, Stamas JN. 1992. Quantification of N-acetyl-L-aspartic acid in urine by isotope dilution gas chromatography-mass spectrometry. *J Inherit Metab Dis* 15:97–104.
- Kitada K, Akimitsu T, Shigematsu Y, Kondo A, Maihara T, Yokoi N, Kuramoto T, Sasa M, Serikawa T. 2000. Accumulation of N-acetyl-L-aspartate in the brain of the tremor rat, a mutant exhibiting absence-like seizure and spongiform degeneration in the central nervous system. *J Neurochem* 74:2512–2519.
- Klugmann M, Symes CW, Klausner BK, Leichtlein CB, Serikawa T, Young D, Doring MJ. 2003. Identification and distribution of aspartoacylase in the postnatal rat brain. *Neuroreport* 14:1837–1840.
- Ledeen RW. 1984. Lipid-metabolizing enzymes of myelin and their relation to the axon. *J Lipid Res* 25:1548–1554.
- Lindner HA, Tafler-Naumann M, Rohm KH. 2008. N-acetyl amino acid utilization by kidney aminoacylase-1. *Biochimie* 90:773–780.
- Ling EA, Kaur C, Lu J. 1998. Origin, nature, and some functional considerations of intraventricular macrophages, with special reference to the ependymal cells. *Microsc Res Tech* 41:43–56.

- Liu J, Casaccia P. 2010. Epigenetic regulation of oligodendrocyte identity. *Trends Neurosci* 33:193–201.
- Madhavarao CN, Arun P, Moffett JR, Szucs S, Surendran S, Matalon R, Garbern J, Hristova D, Johnson A, Jiang W, Namboodiri MA. 2005. Defective N-acetylaspartate catabolism reduces brain acetate levels and myelin lipid synthesis in Canavan's disease. *Proc Natl Acad Sci USA* 102:5221–5226.
- Madhavarao CN, Chinopoulos C, Chandrasekaran K, Namboodiri MA. 2003. Characterization of the N-acetylaspartate biosynthetic enzyme from rat brain. *J Neurochem* 86:824–835.
- Madhavarao CN, Moffett JR, Moore RA, Viola RE, Namboodiri MA, Jacobowitz DM. 2004. Immunohistochemical localization of aspartoacylase in the rat central nervous system. *J Comp Neurol* 472:318–329.
- Matalon R, Michals K, Kaul R. 1995. Canavan disease: From spongy degeneration to molecular analysis. *J Pediatr* 127:511–517.
- Matalon R, Michals K, Sebesta D, Deanching M, Gashkoff P, Casanova J. 1988. Aspartoacylase deficiency and N-acetylaspartic aciduria in patients with canavan disease. *Am J Med Genet* 29:463–471.
- Mehta V, Namboodiri MA. 1995. N-acetylaspartate as an acetyl source in the nervous system. *Brain Res Mol Brain Res* 31:151–157.
- Miyake M, Kakimoto Y, Sorimachi M. 1981. A gas chromatographic method for the determination of N-acetyl-L-aspartic acid, N-acetyl-aspartylglutamic acid and beta-citryl-L-glutamic acid and their distributions in the brain and other organs of various species of animals. *J Neurochem* 36:804–810.
- Moffett JR, Namboodiri MA. 2006. Expression of N-acetylaspartate and N-acetylaspartylglutamate in the nervous system. In: Moffett JR, Tieman SB, Weinberger DR, Coyle JT, Namboodiri MA, editors. *N-Acetylaspartate: A unique neuronal molecule in the central nervous system*. New York, NY: Springer Science + Business Media. pp 7–26.
- Moffett JR, Namboodiri MA, Neale JH. 1993. Enhanced carbodiimide fixation for immunohistochemistry: Application to the comparative distributions of N-acetylaspartylglutamate and N-acetylaspartate immunoreactivities in rat brain. *J Histochem Cytochem* 41:559–570.
- Moffett JR, Ross B, Arun P, Madhavarao CN, Namboodiri AM. 2007. N-Acetylaspartate in the CNS: From neurodiagnostics to neurobiology. *Prog Neurobiol* 81:89–131.
- Namboodiri MA, Moffett JR, Arun P, Mathew R, Namboodiri S, Potti A, Hershfield J, Kirmani B, Jacobowitz DM, Madhavarao CN. 2006. Defective myelin lipid synthesis as a pathogenic mechanism of Canavan disease. In: Moffett JR, Tieman SB, Weinberger DR, Coyle JT, Namboodiri MA, editors. *N-Acetylaspartate: A unique neuronal molecule in the central nervous system*. New York, NY: Springer Science + Business Media. pp 145–163.
- Nave KA. 2010. Myelination and the trophic support of long axons. *Nat Rev Neurosci* 11:275–283.
- Perrier J, Durand A, Giardina T, Puigserver A. 2005. Catabolism of intracellular N-terminal acetylated proteins: involvement of acylpeptide hydrolase and acylase. *Biochimie* 87:673–685.
- Peters A, Palay SL, Webster Hd. 1991. *The fine structure of the nervous system neurons and their supporting cells*, 3rd ed. New York: Oxford University Press.
- Popko B. 2003. Myelin: Not just a conduit for conduction. *Nat Genet* 33:327–328.
- Sakakibara I, Fujino T, Ishii M, Tanaka T, Shimosawa T, Miura S, Zhang W, Tokutake Y, Yamamoto J, Awano M, Iwasaki S, Motoike T, Okamura M, Inagaki T, Kita K, Ezaki O, Naito M, Kuwaki T, Chohnan S, Yamamoto TT, Hammer RE, Kodama T, Yanagisawa M, Sakai J. 2009. Fasting-induced hypothermia and reduced energy production in mice lacking acetyl-CoA synthetase 2. *Cell Metab* 9:191–202.
- Sass JO, Mohr V, Olbrich H, Engelke U, Horvath J, Fliegauf M, Loges NT, Schweitzer-Krantz S, Moebus R, Weiler P, Kispert A, Superti-Furga A, Wevers RA, Omran H. 2006. Mutations in ACY1, the gene encoding aminoacylase 1, cause a novel inborn error of metabolism. *Am J Hum Genet* 78:401–409.
- Sass JO, Olbrich H, Mohr V, Hart C, Woldseth B, Krywawych S, Bjurulf B, Lakhani PK, Buchdahl RM, Omran H. 2007. Neurological findings in aminoacylase 1 deficiency. *Neurology* 68:2151–2153.
- Streit WJ, Graeber MB. 1993. Heterogeneity of microglial and perivascular cell populations: Insights gained from the facial nucleus paradigm. *Glia* 7:68–74.
- Surendran S, Campbell GA, Tyring SK, Matalon R. 2005. Aspartoacylase gene knockout results in severe vacuolation in the white matter and gray matter of the spinal cord in the mouse. *Neurobiol Dis* 18:385–389.
- Takahashi H, McCaffery JM, Irizarry RA, Boeke JD. 2006. Nucleocytoplasmic acetyl-coenzyme a synthetase is required for histone acetylation and global transcription. *Mol Cell* 23:207–217.
- Tallan HH. 1957. Studies on the distribution of N-acetyl-L-aspartic acid in brain. *J Biol Chem* 224:41–45.
- Traka M, Wollmann RL, Cerda SR, Dugas J, Barres BA, Popko B. 2008. Nur7 is a nonsense mutation in the mouse aspartoacylase gene that causes spongy degeneration of the CNS. *J Neurosci* 28:11537–11549.
- Wang J, Leone P, Wu G, Francis JS, Li H, Jain MR, Serikawa T, Ledeen RW. 2009. Myelin Lipid Abnormalities in the Aspartoacylase-Deficient Tremor Rat. *Neurochem Res* 34:138–148.
- Wang J, Matalon R, Bhatia G, Wu G, Li H, Liu T, Lu ZH, Ledeen RW. 2007. Bimodal occurrence of aspartoacylase in myelin and cytosol of brain. *J Neurochem* 101:448–457.
- Wellen KE, Hatzivassiliou G, Sachdeva UM, Bui TV, Cross JR, Thompson CB. 2009. ATP-citrate lyase links cellular metabolism to histone acetylation. *Science* 324:1076–1080.
- Wiame E, Tyteca D, Pierrot N, Collard F, Amyere M, Noel G, Desmedt J, Nassogne MC, Vikkula M, Octave JN, Vincent MF, Courtoy PJ, Boltshauser E, Van Schaftingen E. 2010. Molecular Identification of Aspartate N-acetyltransferase and its Mutation in Hypoacetylaspartia. *Biochem J* 425:127–136.
- Zeng BJ, Wang ZH, Ribeiro LA, Leone P, De Gasperi R, Kim SJ, Raghavan S, Ong E, Pastores GM, Kolodny EH. 2002. Identification and characterization of novel mutations of the aspartoacylase gene in non-Jewish patients with Canavan disease. *J Inherit Metab Dis* 25:557–570.